INELASTIC BEHAVIOUR OF REINFORCED CONCRETE FRAMES DURING EARTHQUAKE

A DISSERTATION SUBMITTED IN PARTIAL FULFILMENT OF THE REQUIREMENTS FOR THE AWARD OF THE DEGREE OF MASTER OF ENGINEERING IN EARTHQUAKE ENGINEERING OF THE UNIVERSITY OF ROORKEE

By
RAVINDRA PRAKASH

SCHOOL OF RESEARCH AND TRAINING IN
EARTHQUAKE ENGINEERING
UNIVERSITY OF ROORKEE
ROORKEE (INDIA)
October, 1973

CERTIFICATE

[redacted]at the thesis entitled "INELASTIC BEHAVIOUR OF REINFORCED CONCRETE FRAMES DURING EARTHQUAKE", which is being submitted by Sri Ravindra Prakash, in partial fulfilment of the requirements for the degree of Master of Engineering in Earthquake Engineering of University of Roorkee, is a record of student's own work carried out by him under my supervision and guidance. The matter embodied in this thesis has not been submitted for the award of any degree or diploma.

This is to further certify that he has worked for a period of nine months from January 1973 to September 1973 for preparing the dissertation of Master of Engineering degree at University of Roorkee.

(BRIJESH CHANDRA)
Reader in Earthquake Engineering
University of Roorkee
Roorkee

Dated: October 13, 1973

Place: Roorkee

SYNOPSIS

The inelastic behaviour of Reinforced Concrete Structures subjected to lateral loads is studied. The values of the strain ductility of the reinforcement and lateral deflection ductility of the portal frame are obtained. An attempt has been made to show the relationship between two ductilities.

The response calculations in the post elastic range are made for two Accelerograms (Koyna and El Centro). The reduction in response due to in-elasticity of the structure is worked out for these two earthquakes and for different deflection ductilities.

ACKNOWLEDGEMENT

The author expresses, with deep gratitude, his sincere thanks to his guide Dr. Brijesh Chandra Mathur, Reader, School of Research and Training in Earthquake Engineering, Roorkee, for his expert guidance and constant encouragement throughout the course of this study.

Author is thankful to Dr. B.C. Mathur for suggesting him the topic of the present study as well as for loaning him the Computer Program for numerical integeration.

Thanks are due to Dr. A.S.Arya, Professor and Head, School of Research and Training in Earthquake Engineering, for the time to time consultations, guidance and encouragement, author sought and received from him.

The computational work was done on IBM 1620 installation at the Structural Engineering Research Centre, Roorkee and on IBM 360/ 44 installation at Delhi University Computer Centre. The author takes this opportunity to thank these organisations for the computer facilities made available to him.

Author thanks his colleagues for the technical discussions he had with them at various stages of the work which proved fruitful.

Thanks are also due to Mr. S.C.Sharma for his help in bringing out the thesis in the present form.

TABLE OF CONTENTS

......

CHAPTER I

INTRODUCTION

It is generally recognized that many structures have successfully resisted the action of major earthquakes although designed to resist much smaller lateral force than those predicted by dynamic elastic considerations. When the elastic response of a typical multistorey-multibay building frame to a major earthquake is calculated, it is evident that the stresses in some of the members are greater than the yield stress of the material. This is because many framed structures are designed on the basis that they will resist more frequent ground motion without damage, but will withstand the most intense seismic shocks without total collapse only by calling on the reserve strength existing beyond the yield deformation point in the individual members. Observation of buildings damaged in earthquakes support the contention that many structures possess an ability to dissipate energy due to inelastic action and thus avoid catastrophic failure under strong motion earthquake loading.

It has been suggested - and it is generally accepted at present - that a seismic design for a building can be based on an elastic analysis made for a reduced acceleration spectra corresponding to a selected value of ductility factor which can be mobilized by the appropriate choice of the structural system. This ductility factor has been usually recommended as 4 to 6 for typical ductile framed structures. However, no attempt has been made to determine whether such a structure can actually achieve this ductility, and further, whether the strains in reinforcement and concrete in the section of the members are within allowable limits at this value of ductility. The present study is an attempt towards getting an insight into the strain behaviour of structural materials vis-a-vis ductility.

A single storey - single bay portal frame is the basic unit of a multistorey - multibay building frame. Also, it is well known that any multi degree freedom system can be made up of number of single degree of freedom systems. For these reasons, a portal frame of the type shown in Fig. 2.4(a) is used for analysis in the present study.

In Chapter II, procedure for finding out the M - ϕ diagram for the column section of the portal frame is outlined. Actual stress-strain relationship for concrete is used and steel is assumed to be elasto-plastic. Using the M - ϕ diagram, a method is indicated to obtain the deflection ductility and the corresponding strains in the reinforcement. Computer programmes for obtaining M - ϕ diagram as well as the ductilities of deflection and strain are given in Appendix A . Curves showing the relation between deflection ductility and the strain ductility are obtained.

Assuming the structure to be elasto-plastic, in Chapter III response calculations of various structural systems to two actual recroded strong-motion accelerograms (Koyna and El Centro) are made. Response reduction factors on account of inelastic behaviour and the associated ductility is examined for a variety of structures.

Chapter IV is concerned with various assumptions and limitations of the present study. The scope of further work in this field is briefly discussed.

Results and conclusions drawn from this study are summarized in Chapter V.

CHAPTER II

COMPUTATION OF DEFLECTIONS

In order to make a rational, nonlinear, dynamic frame analysis, it is necessary to know the appropriate END MOMENT - END ROTATION diagram for the members. From the diagram lateral deflection ductility can be obtained. The strain behaviour of the material of the structure can also be known.

2.1 Moment - curvature relationship

When the frame shown in Fig. 2.4(a) is subjected to a lateral force in one direction, the response may be idealized into three stages of behaviour :

1. The first stage is terminated by cracking of concrete. Theoretically, it should occur when the maximum tensile stress in the section exceeds the modulus of rupture of concrete. Actually, however, cracking is influenced by differential shrinkage stresses and stress concentration at the restraint corners.
2. The second stage is terminated by yielding of the reinforcement. A redistribution of internal stresses after one critical section (in the present case there are four such sections) yields, causes almost immediate

yielding in the remaining cross-sections.

3. The third stage is terminated when the maximum concrete strain in the section reaches the ultimate concrete strain value 'e_{cu}'. After this stage, concrete is crushed and is not supposed to take any more strains.

It is noted that the first stage does not affect the M - ϕ relationship to any appreciable amount. Therefore, for simplicity, only second and third stages may be considered for drawing the M - ϕ diagram. Thus the portion of the M - ϕ curve between the initial stage and the stage when reinforcement yields is considered to be linear. If cracking of concrete is also to be considered, this portion would become bi-linear. The difference between the two is not much as can be seen from Fig. 2.1 in which, for comparison, two M - ϕ diagrams have been plotted for a reinforced concrete section. First diagram is drawn considering the cracking of concrete and second, by ignoring it.

The steel stress-strain relationship is assumed to be elasto-plastic as shown in Fig. 2.2(a). The yield strain of steel e_{sy} is taken equal to 0,0012 and modulus of elasticity of steel E_s is taken equal to $2 \times 10^6 \mathrm{kg/cm^2}$. It can be noted that this is an idealized relationship without considering the strain-hardening effect.

The concrete stress-strain relationship is assumed to be

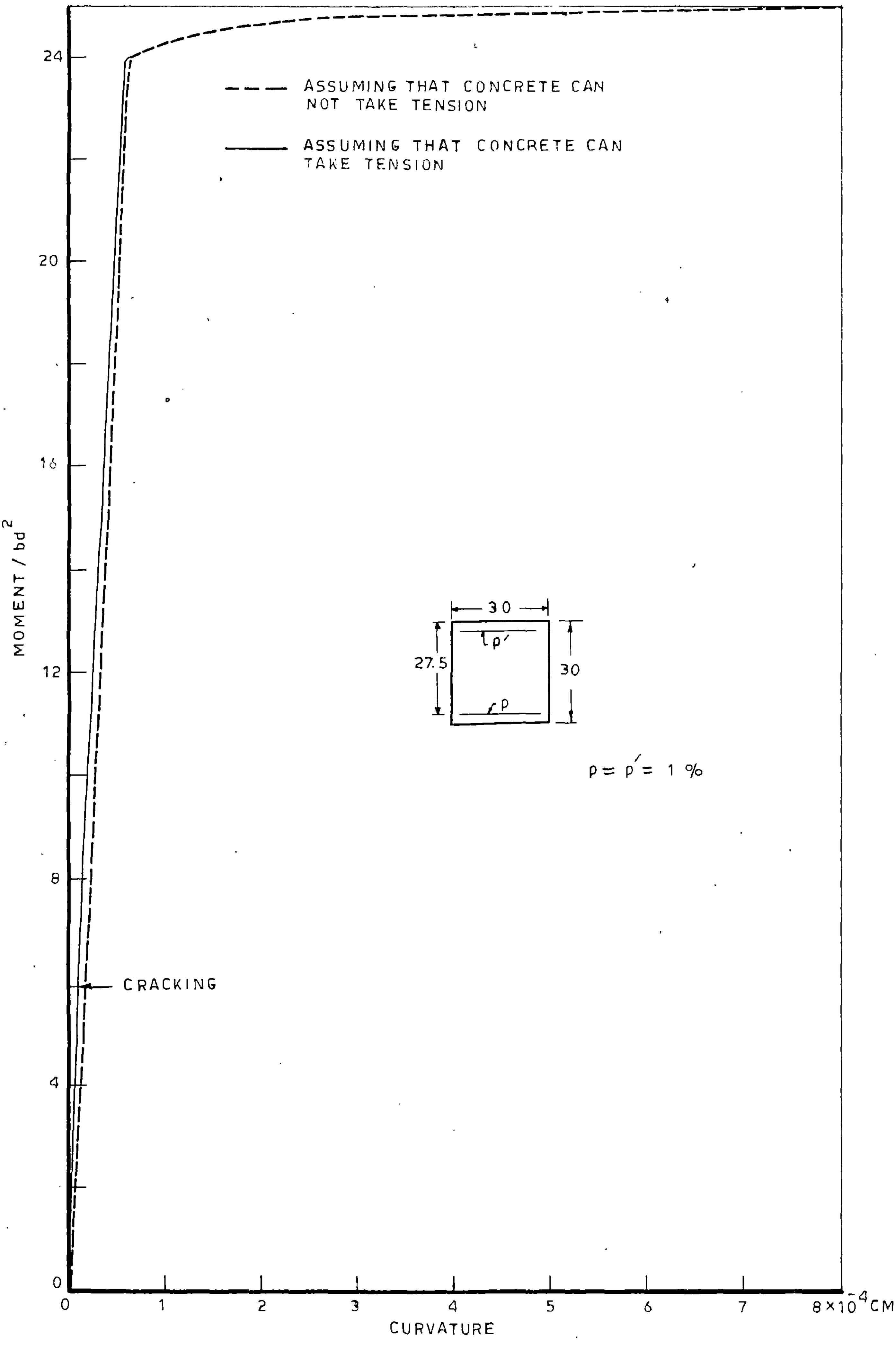
24
20
16
12
8
4
0
MOMENT / bd²
ASSUMING THAT CONCRETE CAN NOT TAKE TENSION
ASSUMING THAT CONCRETE CAN TAKE TENSION
CRACKING
30
27.5
30
ρ′
ρ
ρ = ρ′ = 1 %
0
1
2
3
4
5
6
7
8×10⁻⁴ CM
CURVATURE

FIG. 2.1

parabolic given by the following equation :

$$f = f'_c \left[\left(2 \frac{e}{e_o} - \left(\frac{e}{e_o} \right)^2 \right] \right. \qquad 2.1$$

in which

f = stress in concrete at any instant

e = strain in concrete corresponding to f

e_o = strain in concrete corresponding to the maximum compressive stress f'_c of the concrete.

The plot of the equation is shown in Fig. 2.2(b).

Two sets of computations of elastic deflections have been made for studying the effect of concrete strains e_{cu} and e_o. The values chosen are e_{cu} = .004, e_o = .003; and e_{cu} = .003, e_o = .002.

In addition to the two assumptions made above implicitly, namely, the assumptions regarding the stress-strain relationships of concrete and steel, following additional assumptions are made to simplify computations :

1. Strain in a cross-section is proportional to the distance from neutral axis.
2. The difference of forces of compression and tension in a section is equal to the axial force applied on the section.

3. Internal moment of resistance of the section is equal to the external applied moment.

4. Concrete does not carry any tension.

5. No stresses exist in the concrete or in the reinforcement prior to the start of loading. Hence shrinkage stresses are presumed non-existent.

2.2 Computation of internal forces and moment in the column cross-section

Instead of taking a triangular distribution of stress, the exact stress-strain relationship of concrete based on Equation 2.1 is used to determine the force of compression in concrete. An expression for this force is given below :

Let ' e_c ' denote the strain in the top fibre of concrete. Referring to Figs. 2.2(c), (d) and (e), we can write :

$$e = \frac{e_c}{Nd} . x$$

The force of compression in concrete C_c is then given by

$$C_c = \int_0^{Nd} b.f.dx$$

Substituting for f, integrating, and simplifying, one gets,

$$C_c = \frac{f'_c}{e_o} \cdot \frac{e_c^2}{e_c+e_s} \cdot \left(1 - \frac{e_c}{3e_o}\right) b.d \qquad 2.2$$

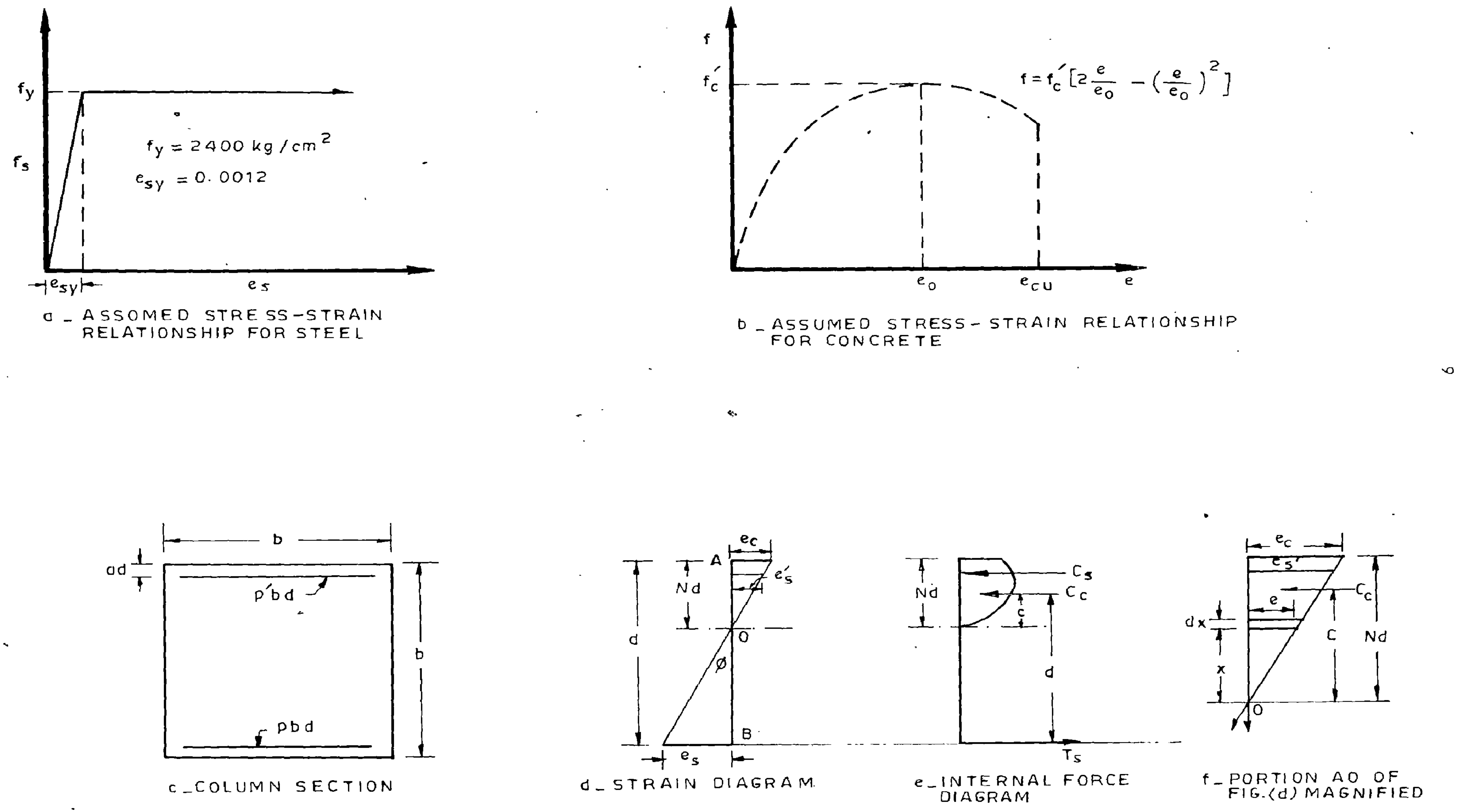

a _ ASSOMED STRESS-STRAIN RELATIONSHIP FOR STEEL

b _ ASSUMED STRESS-STRAIN RELATIONSHIP FOR CONCRETE

c _ COLUMN SECTION

d _ STRAIN DIAGRAM

e _ INTERNAL FORCE DIAGRAM

f _ PORTION AO OF FIG.(d) MAGNIFIED

FIG. 2.2

in which

f'_c = maximum compressive stress of the concrete

b = width of the section

Nd = depth of neutral axis from top fibre

Referring to Figs. 2.2 (a), (c), (d), (e) and (f), the following relationships can be established by consideration of geometry and equilibrium :

$$Nd = \frac{e_c}{e_c + e_s} \cdot d \qquad 2.3$$

$$\phi = \frac{e_c + e_s}{d} \qquad 2.4$$

$$e'_s = (1 - a)\, e_c - a \cdot e_s \qquad 2.5$$

$$C_s = p' E_s e'_s \cdot bd \qquad 0 \leqslant e'_s \leqslant e_{sy} \qquad 2.6(a)$$

$$C_s = p' E_s \cdot e_{sy}\, bd \qquad e'_s \leqslant e_{sy} \qquad 2.6(b)$$

$$T_s = p\, E_s \cdot e_s \cdot bd \qquad 0 \leqslant e_s \leqslant e_{sy} \qquad 2.7(a)$$

$$T_s = p \cdot E_s \cdot e_{sy} \cdot bd \qquad e_s \leqslant e_{sy} \qquad 2.7(b)$$

in which,

e_c = compressive strain in the top fibre of concrete

e_{sy} = yield strain for the steel

d = effective depth of the section

b = width of the section

a.d	=	distance from the top fibre to the centre of compressive reinforcement
E_s	=	modulus of elasticity of steel
e_s	=	strain in the tensile steel
e'_s	=	strain in the compressive steel
ϕ	=	curvature
Nd	=	distance of neutral axis from top fibre
C_s	=	compressive force in the compression steel
T_s	=	tensile force in the tension steel.

Referring to the Fig. 2.2(e), one can obtain the internal moment of resistance by taking moment of C_c and C_s about the centre line of tension steel. Thus,

$$M = C_c . d' + C_s . (1-a) . d \qquad 2.8$$

In the normal linear theory, a triangular stress block of concrete is assumed in which case d' is equal to $(1 - \frac{N}{3})$. In the present case, however, since actual stress-strain relationship of concrete has been used throughout the entire range of loading, an expression for d' is obtained as follows :

From Fig. 2.2(f), taking moment about N.A., the distance of centre of gravity of compressive force from the neutral axis 'c' is given by following expression :

$$c = \frac{\int_0^{Nd} f.x.dx}{\int_0^{Nd} f.dx}$$

Substituting for f, integrating and simplifying,

$$c = \frac{2}{3} . Nd. \frac{(1 - \frac{3}{8} . \frac{e_c}{e_o})}{(1 - \frac{1}{3} . \frac{e_c}{e_o})} \qquad 2.9$$

and $$d' = (1 + c - N) d \qquad 2.10$$

The moment M is the moment at the top of a column. Transferring this moment to the centre line of the beam, we get

$$M_b = M. \frac{h_c + d_b}{h_c} \qquad 2.11$$

in which,

M_b = moment at the centre line of the beam

h_c = clear height of the column

d_b = total depth of the beam

2.3 Equilibrium of Forces

The difference between the compressive force and the tensile force must equal the vertical load plus (or minus in the case of 'tensile' column) the effect of the moment in the top girder. That is,

$$C_c + C_s - T_s = W \pm \frac{2 M_b}{L_b} \qquad 2.12$$

in which L_b is the span of the portal frame and W is the axial force in the column.

2.4 Yielding of Tensile Reinforcement

Using Equations 2.2, 2.6(a), 2.7(b) and 2.12 and replacing e_s by e_{sy}, one obtains,

$$\frac{f'_c}{e_o} \cdot \frac{e_c^2}{e_c + e_{sy}} \left(1 - \frac{e_c}{3 e_o}\right) bd + p' bd E_s \left[(1-a) e_c - a e_{sy}\right]$$

$$- pbd E_s \cdot e_{sy} = W \pm \frac{2 M_b}{L_b} \qquad 2.13$$

This is a rather complex cubic equation in two interdependent unknowns e_c and M_b. Iterative procedure is used to solve such problems. M_b is assumed to be zero for the first cycle and the value of e_c is obtained. With this value of e_c and with the help of Equations 2.2 and 2.3, values of C_c and C_s are obtained. Similarly, from Equation 2.10 d' is obtained. Substituting the values of C_c, C_s and d' in Equation 2.8, value of M is obtained. From M, M_b is given by Equation 2.11 This value of M_b is now used in Equation 2.13 to give new value of e_c and calculations are repeated till by the process of progressive convergence, final value of e_c is obtained. This is thus the value of strain in the top fibre of the concrete when steel yields. This value has been denoted by ' e_{cy} ' to avoid confusion.

In the calculations, minus sign is used for tensile column and W = 0 is used for the case when there is no vertical load on the columns.

If at any stage, it is found that the value of e'_s as obtained from e_c has exceeded the value of e_{sy}, Equation 2.2(b) instead of 2.2(a) is to be used in Equation 2.6.

From this value of e_{cy}, M_{by}, the moment at yield, is obtained with the help of Equations 2.2, 2.3, 2.8 and 2.11. Curvature at yield is given by

$$\phi_y = \frac{e_{cy} + e_{sy}}{d}$$

Thus the yield point on the M - ϕ diagram is established.

2.5 Ultimate condition

In this case, the value of e_c is a known priori namely equal to e_{cu}, while strain in steel 'e_s' is unknown. Using e_{cu} in place of e_c in Equation 2.13 an equation quadratic in e_s is obtained. Again this equation is solved by iterative process putting M_b equal to zero in the right hand side for the first cycle approximation. Identical procedure as explained earlier for obtaining the yield point is followed and the value of e_s at ultimate is obtained. Denoting this value of e_s by e_{su} and using Equations 2.2, 2.3, 2.8 and 2.11, value of M_{bu} is obtained. Curvature at ultimate is given by

$$\phi_u = \frac{e_{cu} + e_{su}}{d}$$

This gives the point corresponding to ultimate condition on the M - ϕ diagram.

The three significant points namely, the origin, the yield point and the point corresponding to ultimate condition on the M - ϕ diagram are thus obtained. Other points on the diagram are found by assigning values to e_c between zero and e_{cy} and between e_{cy} and e_{cu}. Complete M - ϕ diagram is thus obtained.

A computer programme is written for obtaining the M - ϕ diagram. The programme can accommodate variation in almost any parameter. Besides giving the values of moment and curvature, the programme also gives values of strain in steel, both tensile and compressive, values of strain in the top fibre of concrete, position of N.A. and the values of 'j'. For reference purposes, a listing of this programme is given in Appendix A.

2.6 The structure chosen for study

For the purpose of study, a portal frame of the dimensions shown in Fig. 2.4(a) is chosen. Different parameters and their values chosen for study are as follows :

1. Both height h_c and span L_b of the frame is taken equal to three metres.
2. Three square sections of columns are taken of sides 20 cms, 25 cms and 30 cms.

3. The beam is supposed to be infinitely rigid in comparison to the columns.

4. The section of beam is taken as a 20 x 30 rectangular section.

5. Ratio of compressive and tensile steel is kept equal to unity as it is the normal practice in an earthquake resistent design, the direction of the anticipated motion being unknown.

6. Studies are made for four different percentages of steel in the section namely, equal to 1.0 %, 1.5 %, 2.0 % and 2.5 % of the column section at each face.

7. Three different types of concrete made use of in the study are M 150, M 200 and M 250.

The ultimate strain of concrete e_{cu} and the strain at which compressive stress is maximum e_o, are also varied. The study is made using $e_{cu} = 0.004$ and $e_o = 0.003$ but one set of computation has been made using $e_{cu} = 0.003$ and $e_o = 0.002$.

8. The direct thrust on each column is kept equal to 4,000 kgs. This value has been arrived at by assuming the live load equal to 400 kgs/cm^2 and by keeping the slab thickness equal to 10 cms. The portal frames are assumed to be 4 metres apart.

2.7 Calculation of deflections

Having obtained the M - ϕ relationship for a particular column section, the next step is to obtain the lateral deflections of the portal frame at each stage of loading. The deflection corresponding to a given curvature is found by integrating curvature over the free height of the column. This is done as follows:

The column is considered in two distinct portions. One which is always elastic and the other, which can yield. Taking both the column bases as rigid and assuming the beam to be infinitely rigid in comparison to the columns it can be seen, using the notations as defined in Figs. 2.4(b) and (d), that the lateral deflection X of the structure is equal to

$$X = 2\left[l_2 \sin(\theta_1 + \theta_2) - Y_2 \cos(\theta_1 + \theta_2) + Y_1\right] \qquad 2.14$$

in which θ_1, θ_2, l_1, l_2, Y_1 and Y_2 are as shown in Figs. 2.4(b) and (d). θ_1 and Y_1 are the only terms affected by yielding.

Assuming the bending moment distribution as shown in Fig.2.4(b), Y_2 and θ_2 can be obtained as follows :

$$\theta_2 = \int_A^B \phi(z).\, dz$$

and

$$Y_2 = \int_A^B \phi(z).\, z.\, dz$$

where z is measured from A in Fig. 2.4(d).

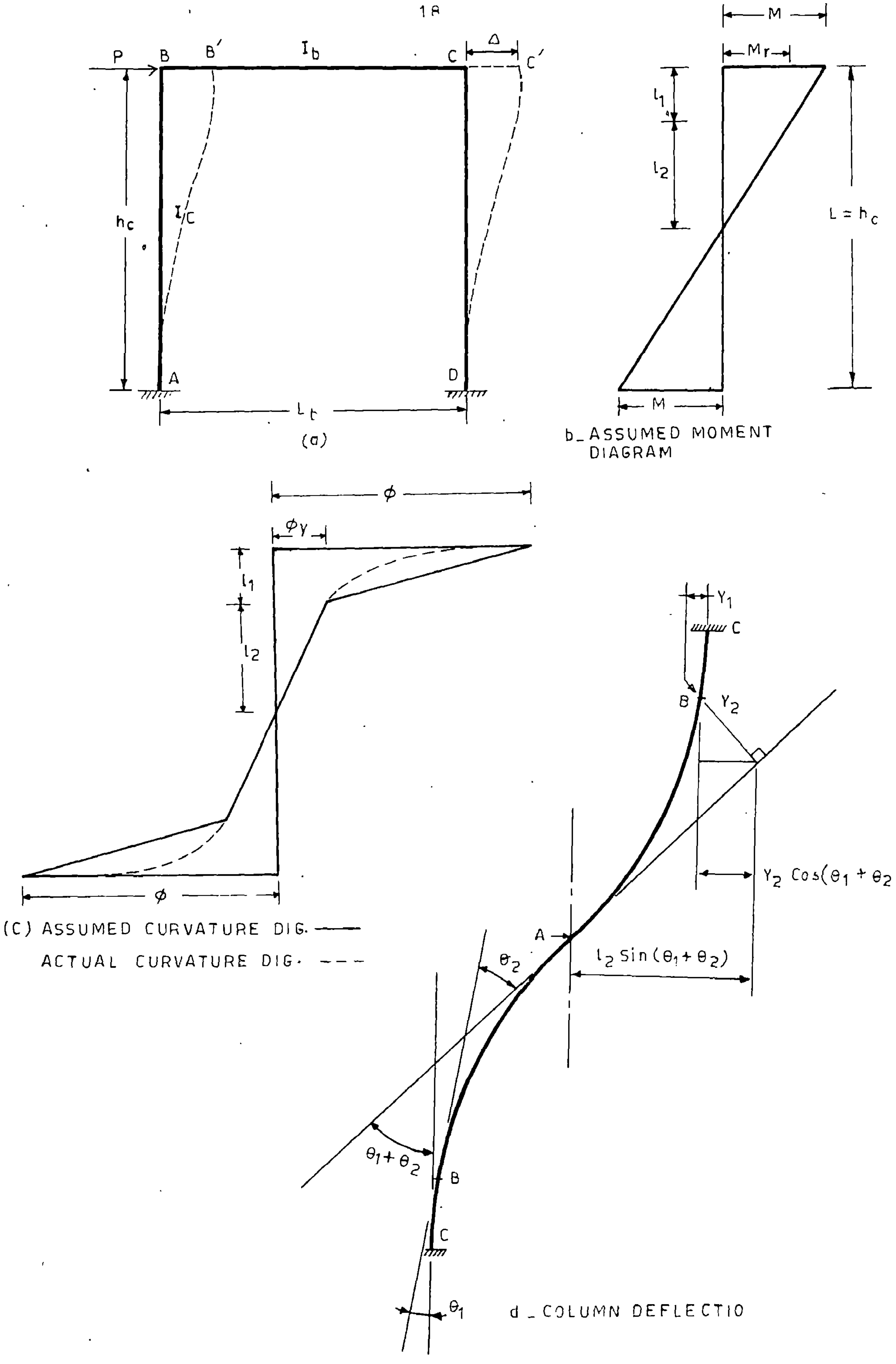

P
B
B′
I_b
C
Δ
C′
h_c
I_c
A
D
L_t
(a)
M
Mr
l_1
l_2
$L = h_c$
M
b_ASSUMED MOMENT DIAGRAM
φ
φy
l_1
l_2
φ
(C) ASSUMED CURVATURE DIG. ———
ACTUAL CURVATURE DIG. - - -
Y_1
C
B
Y_2
$Y_2 \cos(\theta_1 + \theta_2$
A
θ_2
$l_2 \sin(\theta_1 + \theta_2)$
$\theta_1 + \theta_2$
B
C
θ_1
d _ COLUMN DEFLECTIO

FIG. 2.4

θ_1 is equal to the sum of all elemental curvatures occurring from B to C or,

$$\theta_1 = \int_B^C \phi(z)\, dz$$

and again

$$Y_1 = \int_B^C \phi(z).\, z.\, dz$$

where z is measured from B in Fig. 2.4(d).

Substituting for $\phi(z)$ from Figs. 2.4(c) and (d), integrating and simplifying one can obtain the values of the above integrals as given below :

$$\theta_2 = \frac{\phi_y \cdot l_2}{2} \qquad 2.15$$

$$Y_2 = \frac{\phi_y \cdot l_2^2}{3} \qquad 2.16$$

$$\theta_1 = \frac{l_1}{2} (\phi + \phi_y) \qquad 2.17$$

and

$$Y_1 = \frac{l_1^2}{6} (2\phi + \phi_y) \qquad 2.18$$

It should be noted that in the calculations for θ_1 and Y_1 the variation of curvature from ϕ_y to ϕ_u is assumed linear as shown in Fig. 2.4(c). This is done for the sake of simplicity only. Actually, however, the variation in the curvature from ϕ_y to ϕ_u is asymptotic in nature as shown by dotted lines in Fig. 2.4(c).

From Fig. 2.4(b),

$$l_2 = \frac{L}{2} \cdot \frac{M_y}{M}$$

and $$l_1 = \frac{L}{2} - l_2$$

With the help of Equation 2.14 the value of lateral deflection X corresponding to any given moment can now be obtained. The lateral force corresponding to this moment is obtained from

$$P = \frac{4\,M}{h_c}$$

The M - ϕ diagrams for the three sections chosen for study are given in Fig. 2.3.

A plot of load deflection curve is given in Fig. 2.5 for two representative column sections chosen.

2.8 Calculations of deflection ductility and strain ductility

Dividing the lateral deflections by the corresponding values at yield, deflection ductility ratio 'D' is obtained. Again, dividing the strains in the tensile steel by the yield strain of the steel, the strain ductility is obtained.

A computer programme is written to compute deflection ductility and strain ductility. The programme also gives the values of lateral load, lateral deflection, the ratio M/M_y and the ratio ϕ/ϕ_y at each stage of loading. A listing of the programme is given in Appendix A for reference.

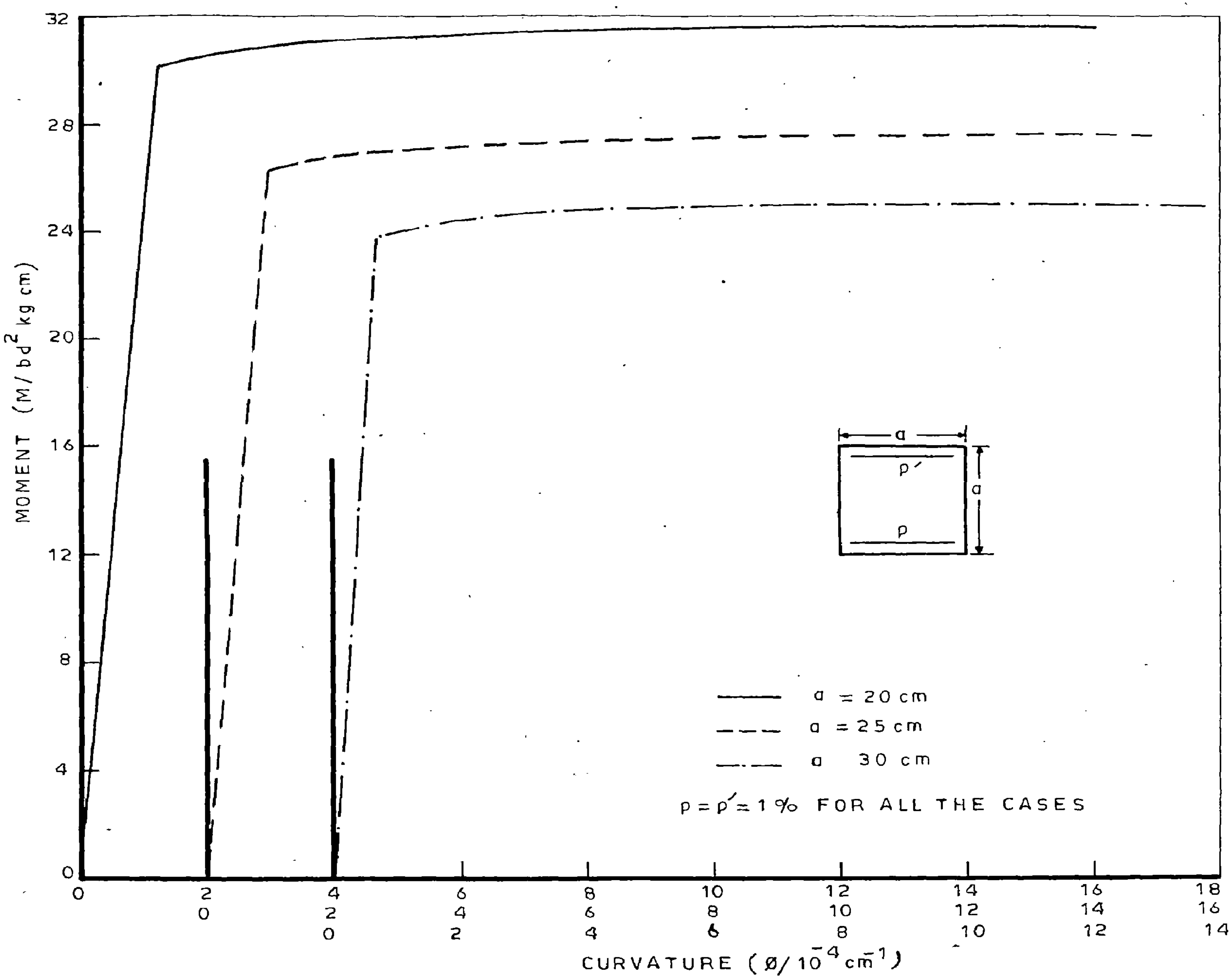

FIG. 2.3_TYPICAL M–Φ DIAGRAMS

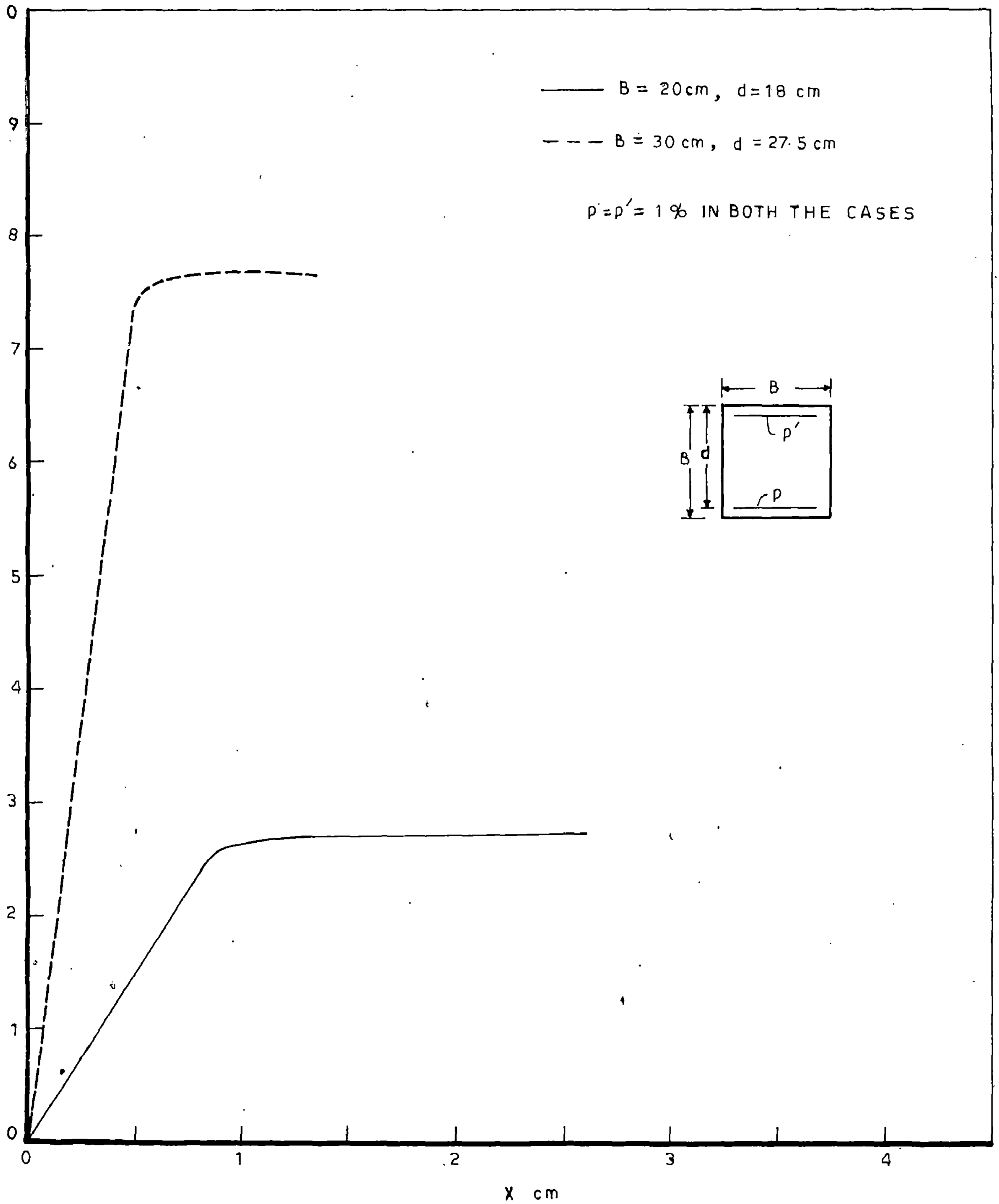

FIG. 2.5 _ TYPICAL LOAD - DEFLECTION PLOTS

2.9 Presentation of results

For a particular set of parameters, it is found that the tensile column always yields earlier than the compression column. Hence the computation of deflections is made on the basis of M - ϕ diagram obtained for tensile columns.

2.9.1 It is readily seen from Fig. 2.1 that the M - ϕ diagram for a given cross section more or less remains unaffected by assuming that concrete does not carry any tension. This plot therefore, proves the validity of the corresponding assumption made in the present study.

2.9.2 The effect of direct thrust on the column moments is shown in Table 2.1. It can be seen that the vertical load on the column has small but appreciable effect on the yield moment and ultimate moment of the column section.

2.9.3 In order to provide a clear picture of the yielding behaviour of a system, it is necessary to study the plot of deflection ductility of the system versus the strain ductility of the steel of a critical R.C.C. section forming a part of the system. In the present study of portal frame, such a representative cross-section is of the tensile column. These plots are given in Figs. 2.6(a) and 2.7(a).

In both the cases, it is seen that the plots are bilinear and that the ratio of maximum deflection to the yield deflection is of the order of 3. However, a glance at the abscissa reveals that at such a

TABLE 2.1 EFFECT OF DIRECT THRUST ON COLUMN MOMENTS

p = p' in all cases

ONLY DL ACTING

p (in %)	M_y (x bd^2 kg-cm) Tension	Comp.	M_u (x bd^2 kg-cm) Tension	Comp
0.5	11.32	17.05	11.84	18.43
1.0	21.22	31.88	22.01	34.22
1.5	31.16	46.89	32.19	50.01
2.0	41.15	62.06	42.34	65.69
2.5	51.17	77.34	52.52	81.26

DL + 50 % LL

p (in %)	M_y Tension	M_y Comp.	M_u Tension	M_u Comp
0.5	12.09	18.17	12.65	19.68
1.0	21.98	33.00	22.83	35.47
1.5	31.93	48.01	33.00	51.23
2.0	41.92	63.19	43.17	66.87
2.5	51.95	78.49	53.32	82.40

DL + FULL LL

p (in %)	M_y Tension	M_y Comp.	M_u Tension	M_u Comp
0.5	12.85	19.28	13.46	20.96
1.0	22.74	34.11	23.63	36.72
1.5	32.69	49.14	33.80	52.44
2.0	42.69	64.32	43.97	68.04
2.5	52.71	79.62	54.12	83.53

value of deflection ductility, the strain ductility is between 20 and 24. This is indeed a very high value. The steel at this stage can not be trusted to perform its function (of carrying the tensile stress) properly. The maximum value of strain ductility which can be tolerated is around seven. The ordinate at this value of strain ductility in both the cases is of the order of 1.5. This value therefore, appears to be the maximum value of deflection ductility which can be safely adopted for earthquake resistant design of the structures used in the present study.

2.9.4 Figs. 2.6(a) and 2.7(a) also reveals effect of the percentage of steel on the $\frac{X}{X_y}$ Vs. $\frac{e}{e_y}$ plot. In both the cases, it is seen that for the same value of $\frac{e}{e_y}$, the value of $\frac{X}{X_y}$ decreases with the increase in the percentage of steel. The non-linear behaviour and hence the ductility of the structure being an important criterion in an earthquake resistant design, it therefore, becomes imperative to have minimum amount of steel which can be used without affecting the strength of the section. In other words, over reinforced sections are to be avoided.

2.9.5 The plot of $\frac{X}{X_y}$ Vs. $\frac{\phi}{\phi_y}$ given in Figs. 2.6(a) and 2.7(a) shows that the relationship between them is also bilinear and that an increase in the amount of steel decreases the value of $\frac{X}{X_y}$ for the same value of $\frac{\phi}{\phi_y}$.

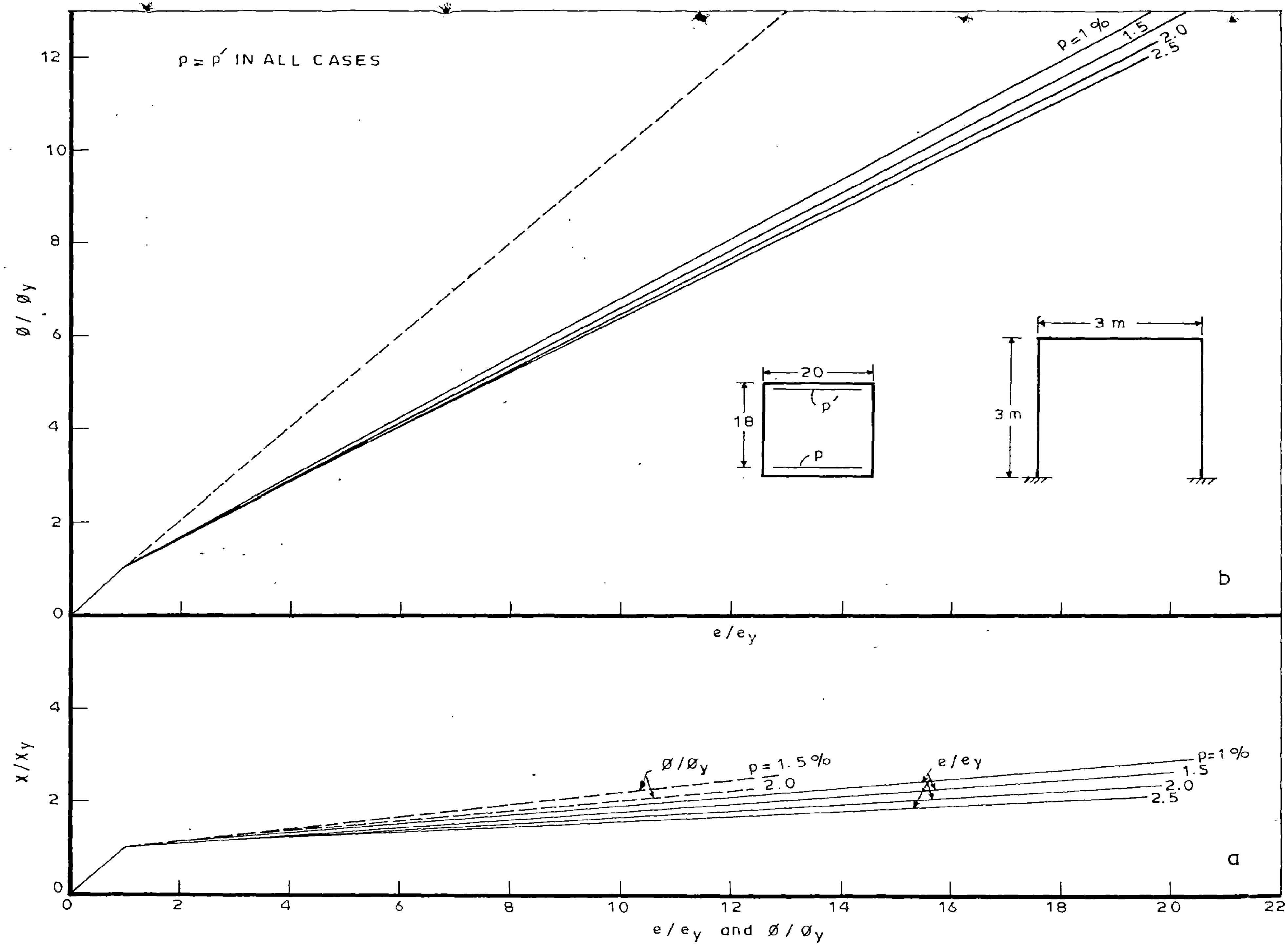

p = p′ IN ALL CASES
p=1%
1.5
2.0
2.5
20
18
p′
p
3 m
3 m
b
ø / øy
e / ey
a
χ / χy
ø / øy
p = 1.5%
2.0
e / ey
p=1%
1.5
2.0
2.5
0
2
4
6
8
10
12
14
16
18
20
22
e / ey and ø / øy

FIG. 2.6

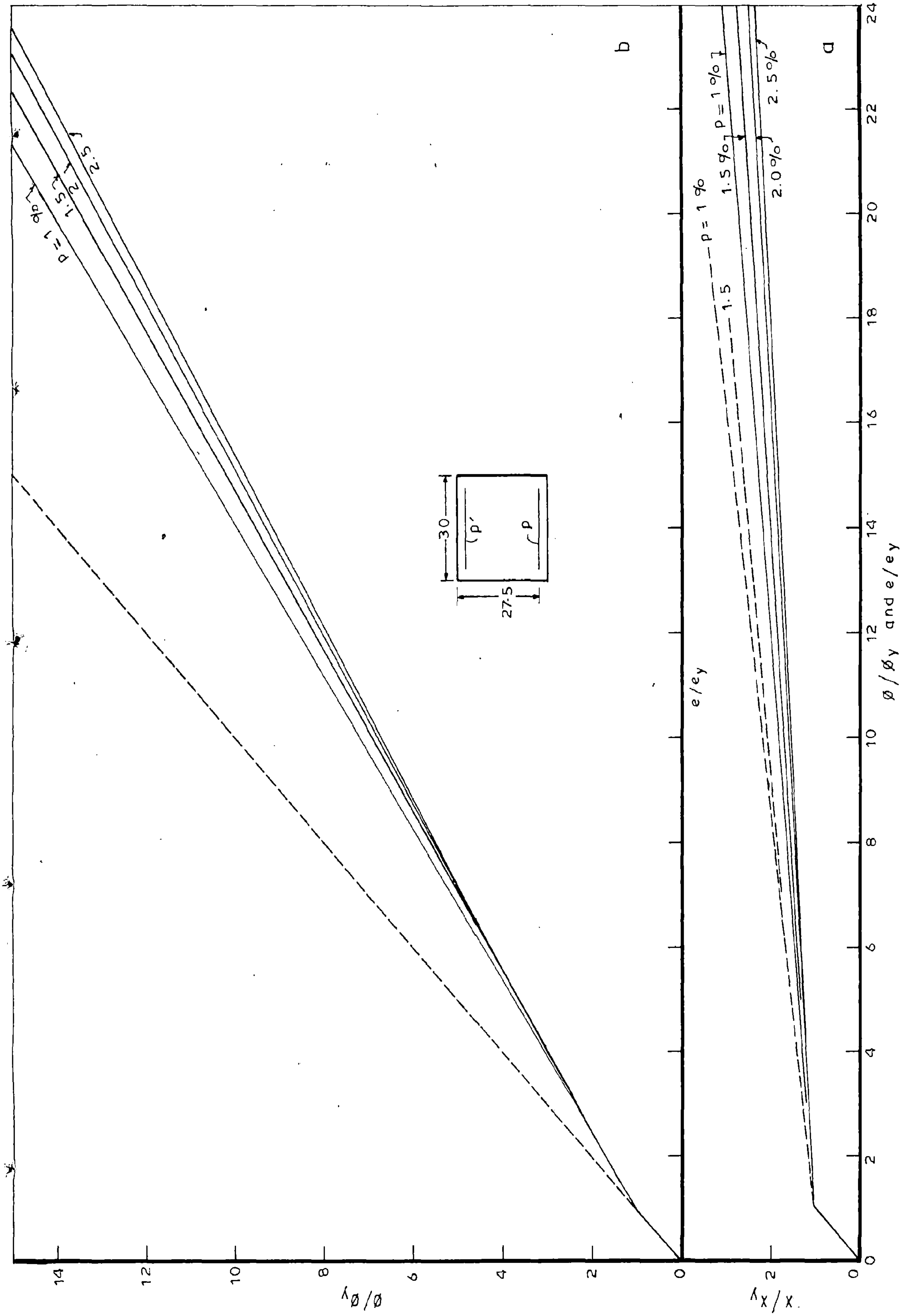

FIG. 2. 7

2.9.6 Depicted on Figs. 2.6(b) and 2.7(b) are plots between curvature ductility $\frac{\phi}{\phi_y}$ and strain ductility $\frac{e}{e_y}$. These two plots are also bilinear. However, the deviation from linear is less pronounced than in the case of $\frac{X}{X_y}$ Vs. $\frac{e}{e_y}$ and $\frac{X}{X_y}$ Vs. $\frac{\phi}{\phi_y}$ plots. Increase in the percentage of steel decreases the value of $\frac{\phi}{\phi_y}$ for the same value of $\frac{e}{e_y}$.

2.9.7 Fig. 2.8 shows the effect of change of maximum compressive stress of concrete on the plot of $\frac{X}{X_y}$ Vs. $\frac{e}{e_y}$. The curves are given for three types of concrete namely, M 150, M 200 and M 250, and for four percentages of steel of 1 %, 1.5 %, 2.0 % and 2.5 % on each face of the cross-section. The section chosen for the comparison is square of side equal to 30 cms. It can be noted from these plots that richer the mix, more is the deflection ductility for the same value of strain ductility and for the same value of steel.

2.9.8 The effect of change in the values of e_o and e_{cu} on $\frac{X}{X_y}$ Vs. $\frac{e}{e_y}$ plot can be seen from Fig. 2.9. The plots have been made taking e_{cu} = .004, e_o = 0.003 and e_{cu} = 0.003, e_o = 0.002. Percentages of steel are kept 1 %, 1.5 %, 2 % and 2.5 %. Section chosen is square of side 30 cms. It can be noted that for p = 1.5 % and p = 2.0 %, the two curves belonging to two sets of values of e_{cu} and e_o are almost overlapping. For p = 1.0 % and 2.5 %, the two curves differ very slightly. It is, therefore, infered that the value of e_{cu} and e_o do not affect the $\frac{X}{X_y}$ Vs. $\frac{e}{e_y}$ plot to any appreciable amount.

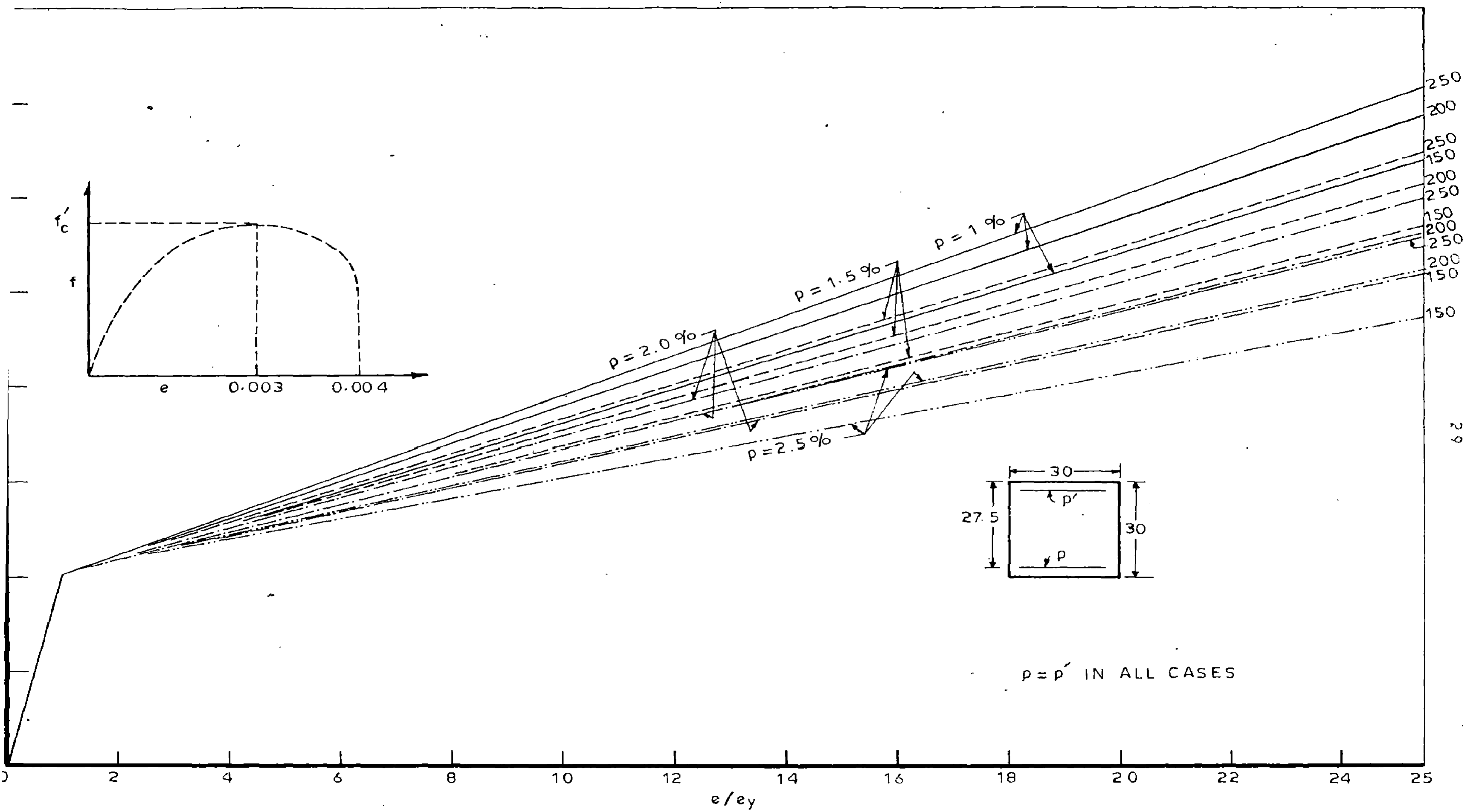

FIG. 2.8 – EFFECT OF CHANGE OF MAXIMUM COMPRESSIVE STRESS OF CONCRETE ON DUCTILITY RATIO

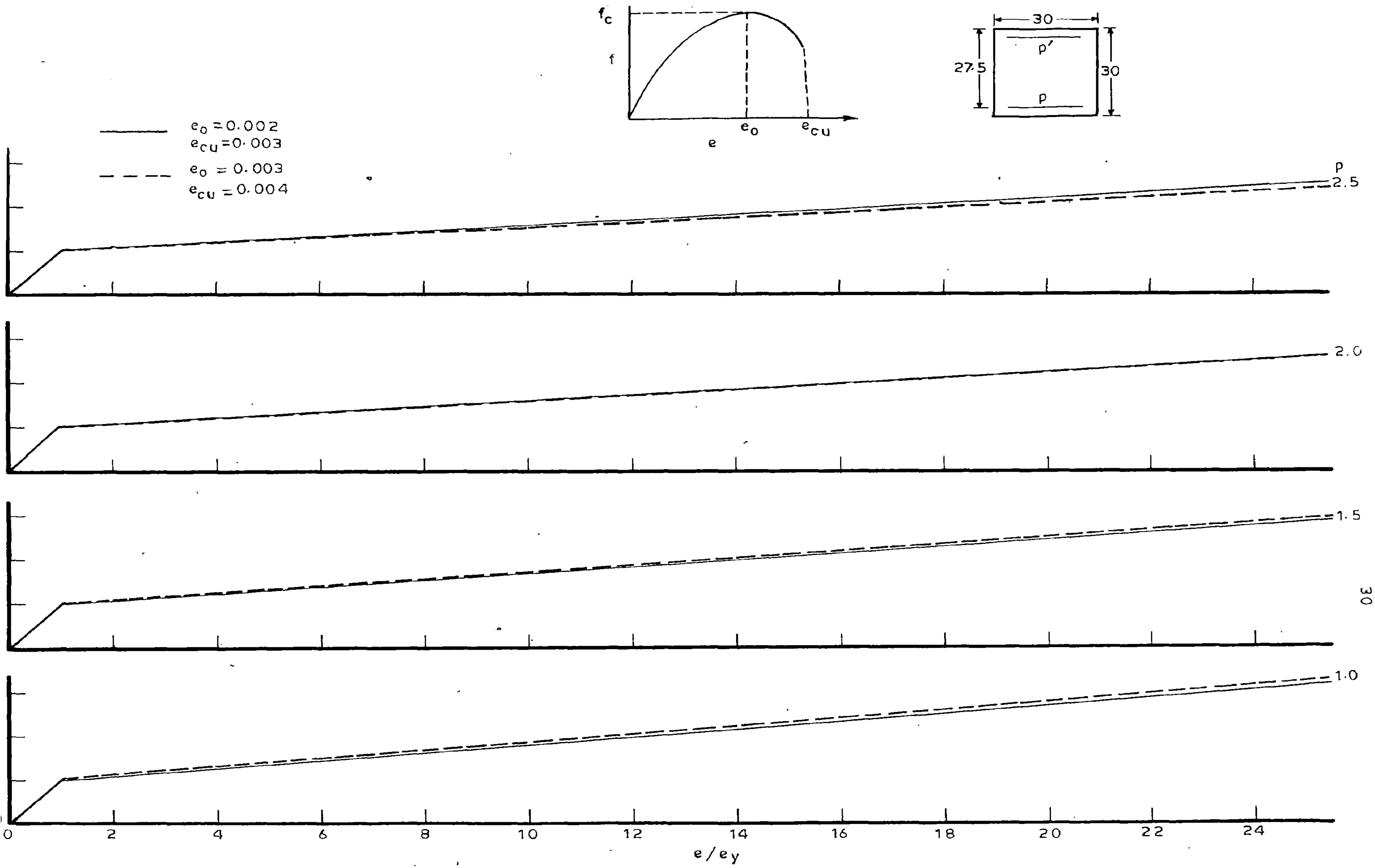

f_c
f
e
e_o
e_cu
30
27.5
30
p'
p
e_o = 0.002
e_cu = 0.003
e_o = 0.003
e_cu = 0.004
p
2.5
2.0
1.5
1.0
0
2
4
6
8
10
12
14
16
18
20
22
24
e/e_y

FIG. 2.9

CHAPTER III

RESPONSE OF ELASTIC AND ELASTO-PLASTIC SYSTEMS TO EARTHQUAKE EXCITATION

A structural system may fail in two ways viz. functional failure and structural failure. If the system though structurally sound, is no longer able to perform its function for which it is originally designed, it is said to have failed functionally. On the other hand, if the system is unable to take the design loads, it is said to have failed structurally.

It has been noted during past earthquakes that many structures, in the event of an earthquake, were able to withstand, without much damage, much higher earthquakes than what they were originally designed for. The reason is not far to seek. The structures generally are designed assuming them to be linear. During an earthquake, the reserve potential of strength which lies in the non-linear range, comes to the rescue of the structure. In other words, keeping the non-linear behaviour of the structures in mind, it is possible to design them elastically for reduced forces. In the event of an actual earthquake such a structure, though it may fail functionally, will at least, not collapse. Non-linearity thus ensures economy in design, as well as safety of life and property. It is important, therefore, to study the behaviour of structural systems in non-linear range. In what follows, an attempt has been made to examine the dynamic response of elastic and elasto-plastic structural systems subjected to ground motions. Two different earthquakes viz. Koyna earthquake of December 11, 1967 and ElCentro earthquake of May 18, 1940 have been chosen for the purpose of this study.

3.1 Equation of motion for a S.D.F. non-linear system

The equation of motion for a single degree freedom non-linear system is

$$m\ddot{x} + c\dot{x} + R(x) = -m\ddot{y}(t) \qquad 3.1$$

in which,

m	=	mass of the system
x	=	relative displacement of the system with respect to ground
c	=	damping
R	=	restoring force function
y	=	ground displacement
t	=	time parameter

and dots denote differentiation with respect to time.

Dividing Equation 3.1 by m, we get,

$$\ddot{x} + 2\xi p\dot{x} + \frac{1}{m}.R(x) = -\ddot{y}(t) \qquad 3.2$$

The restoring force versus deflection curve has been assumed to be elasto-plastic in nature and is shown in Fig. 4.1(b).

With this form of restoring force characteristics it is possible to describe the system by its frequency p, damping ρ and the maximum force level R_y. Also it is convenient to express the maximum force level in terms of acceleration $a_y = \frac{R_y}{m}$. a_y expressed as a function of 'g' is called the yield level of the structure.

The Equation 3.2 is solved on a IBM 360/44 model digital computer, using Runge-Kutta fourth order procedure of numerical integration.

3.2 Reduction factor

At this stage, it is possible to introduce the concept of REDUCTION FACTOR. As the name suggests, the term reduction factor, hereafter denoted as R.F. for brevity, is the ratio of the maximum force attracted by a linear system and the maximum force reached in the same system if it were to become plastic at a particular yield level. In other words, reduction factor is a factor by which the intensity of the earthquake motion may be scaled down so that a linear analysis with the reduced ground motions corresponds to the non-linear analysis with actual ground motions. Therefore, if a system goes into the inelastic range then R.F. is given by

$$RF = \frac{a_m}{a_y}$$

where, a_m = maximum acceleration for the system if it were linear.

3.3 Response computations

Six different systems are analysed for response to two accelerograms viz. longitudinal component of Koyna earthquake and N-S component of ElCentro earthquake. The systems chosen have periods equal to 0.10, 0.20, 0.50 and dampings equal to 10 % and 20 % of critical damping. The computer programme works out the values of maximum relative displacements, ductility, and the maximum accelerations for a particular system defined by γ , T, and q_y . The value of q_y is varied from 0.05 to 1.0.

The accelerograms for two earthquakes selected for study are given in Figs. 3.1 and 3.2.

3.4 Presentation of results

Figs. 3.3 to 3.6 gives a plot for ductility ratio versus reduction factor for two accelerograms viz. Koyna earthquake of December 11, 1967 and ElCentro earthquake of May 18, 1940. Following inferences can be drawn from these figures.

3.4.1 The reduction factor always increases with an increase in ductility for a given damping and given time period of the system.

3.4.2 The rate of increase of RF with ductility is larger for larger periods of the system. In other words, for a given damping and given accelerogram the plot between ductility and reduction factors becomes less steep for larger periods.

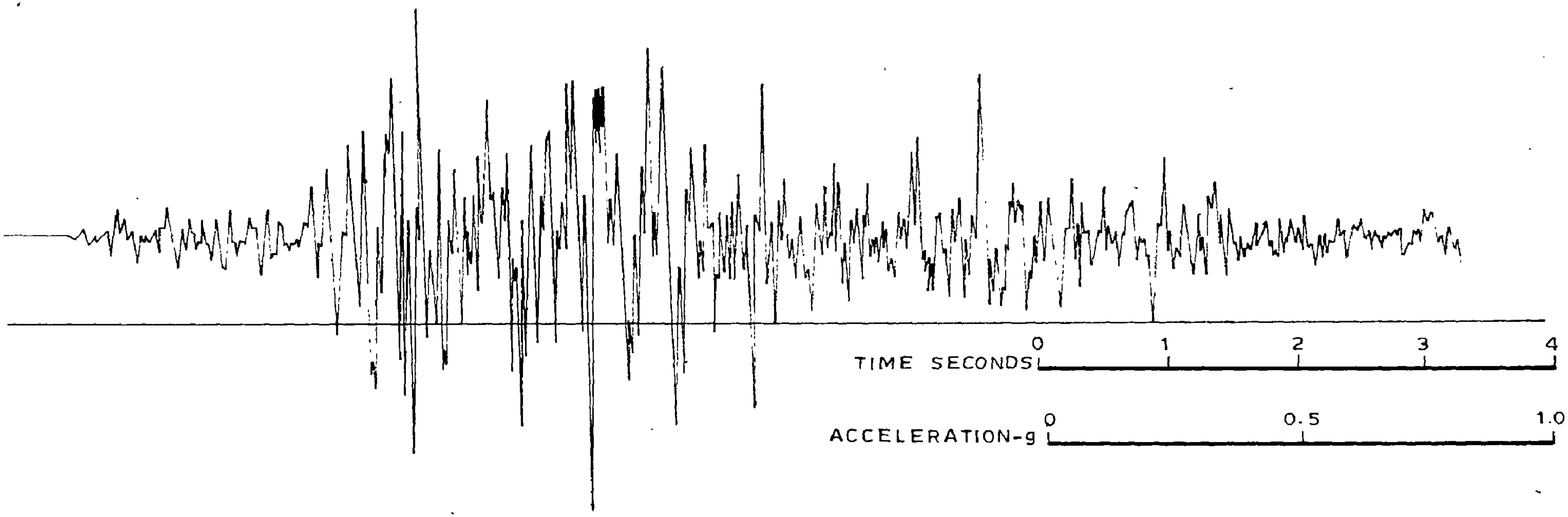

FIG.3.1 – ACCELEROGRAM OF KOYNA EARTHQUAKE OF DEC. 11 1967 AT 04.21 HOURS
ACC. NO. 111

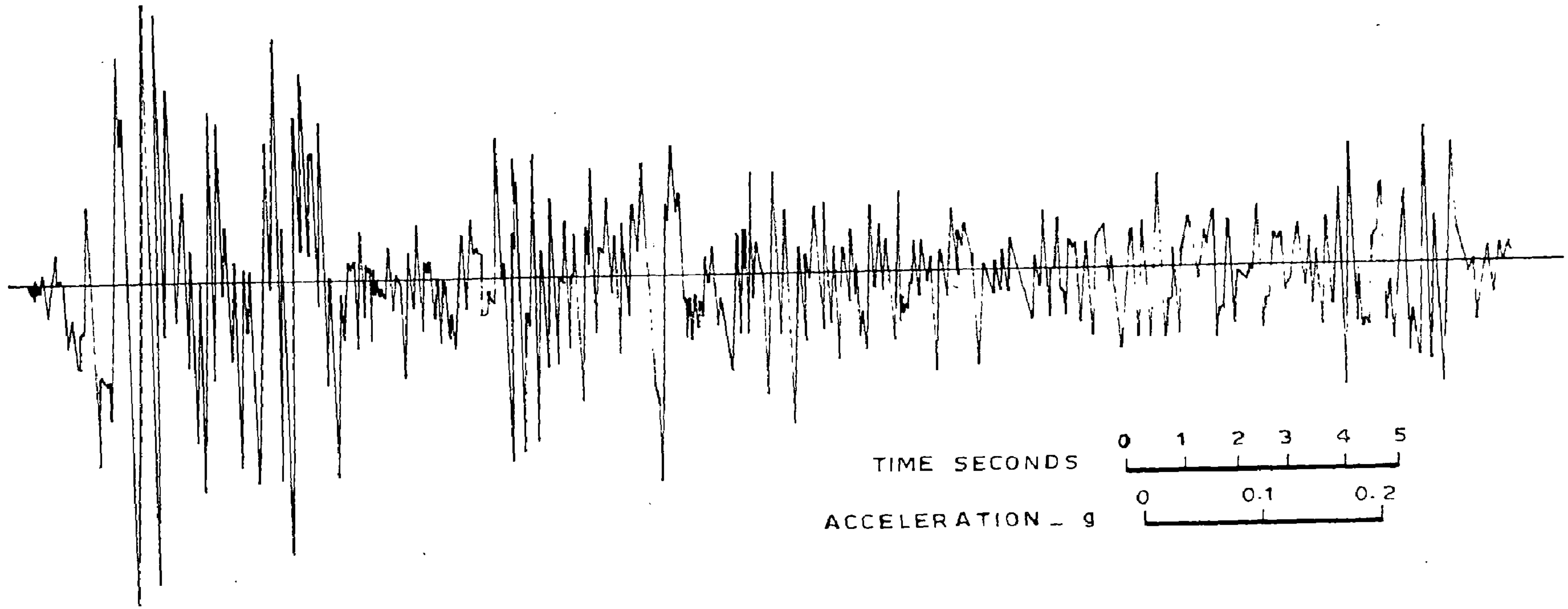

FIG.3.2 _ ACCELEROGRAM OF EL CENTRO SHOCK OF MAY 18, 1940 ACC. NO. 102

3.4.3 Figs. 3.3 to 3.6 also gives plots between RF and period of vibration of the system for different dampings and for different ductility ratios for both the earthquakes. It is noted that for the Kyona earthquake, the reduction factor increases with period in the low ranges of period and decreases with period in higher ranges of period.

For ElCentro earthquake however, such is not the case. Here, the reduction factor increases with an increase in the period. The increase is low in the lower ranges of period and high in the higher ranges of the period.

This shows that reduction factor is very closely associated with ground motion.

3.4.4 It can be seen from Fig. 3.7 that for a particular period and damping, the ductility ratio is higher for lower yield levels. Also it is noted that the ductility ratio does not vary with the period in the same manner for two accelerograms. For El Centro, the ductility ratio increases with period for short periods and decreases for long periods. For Kyona, ductility ratio decreases with increasing periods. Thus no uniform pattern can be established. The choice of the minimum yield level chosen for design will, therefore, depend upon the particular accelerogram and particular ductility chosen for design.

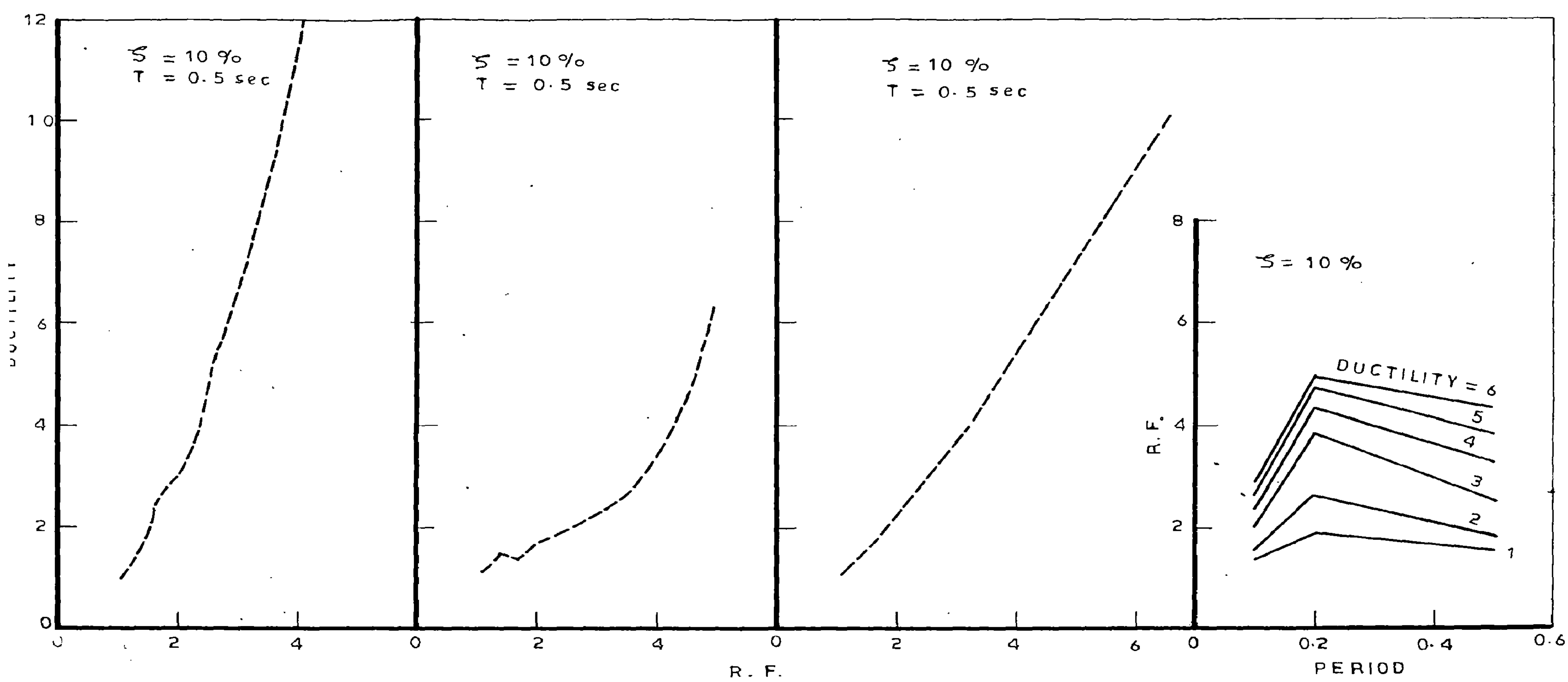

FIG.3.3_ KOYNA EARTHQUAKE

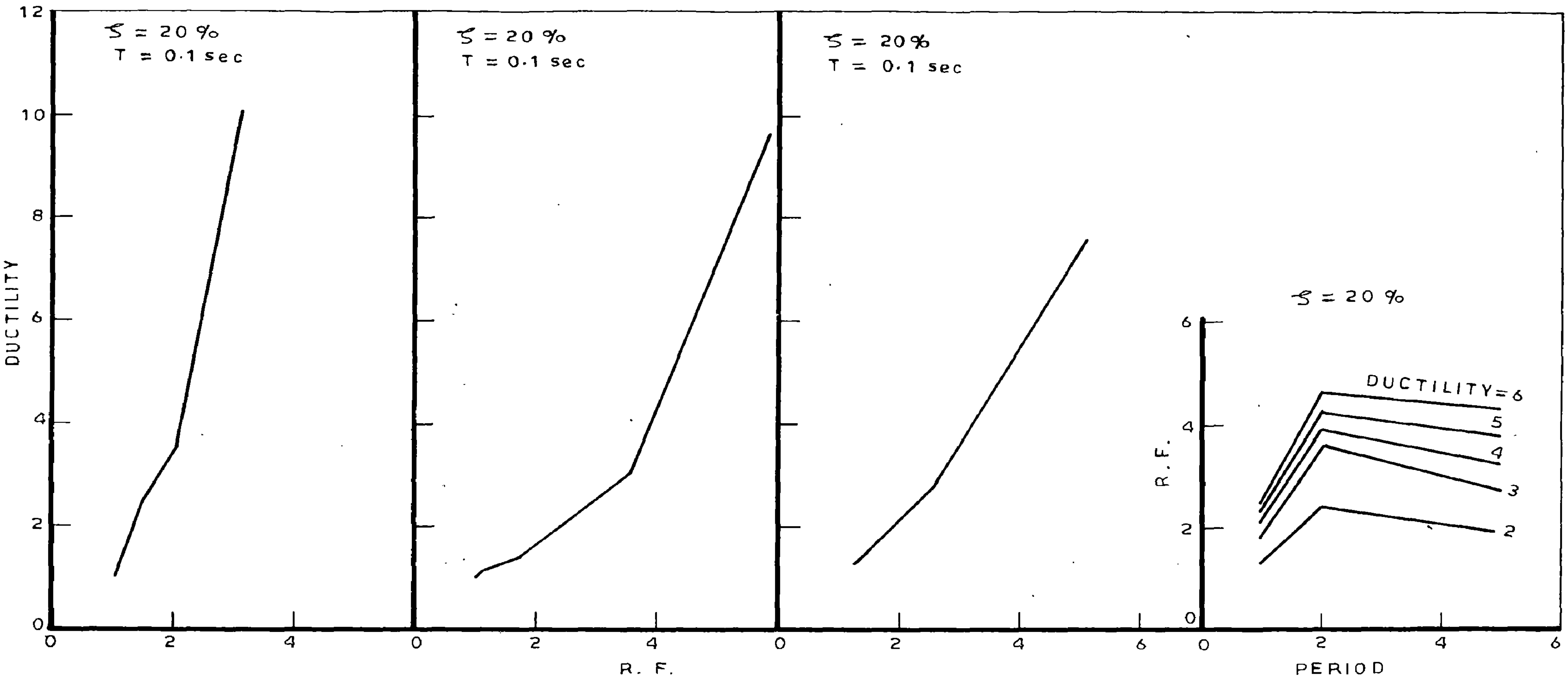

FIG. 3.4 _ KOYNA EARTHQUAKE

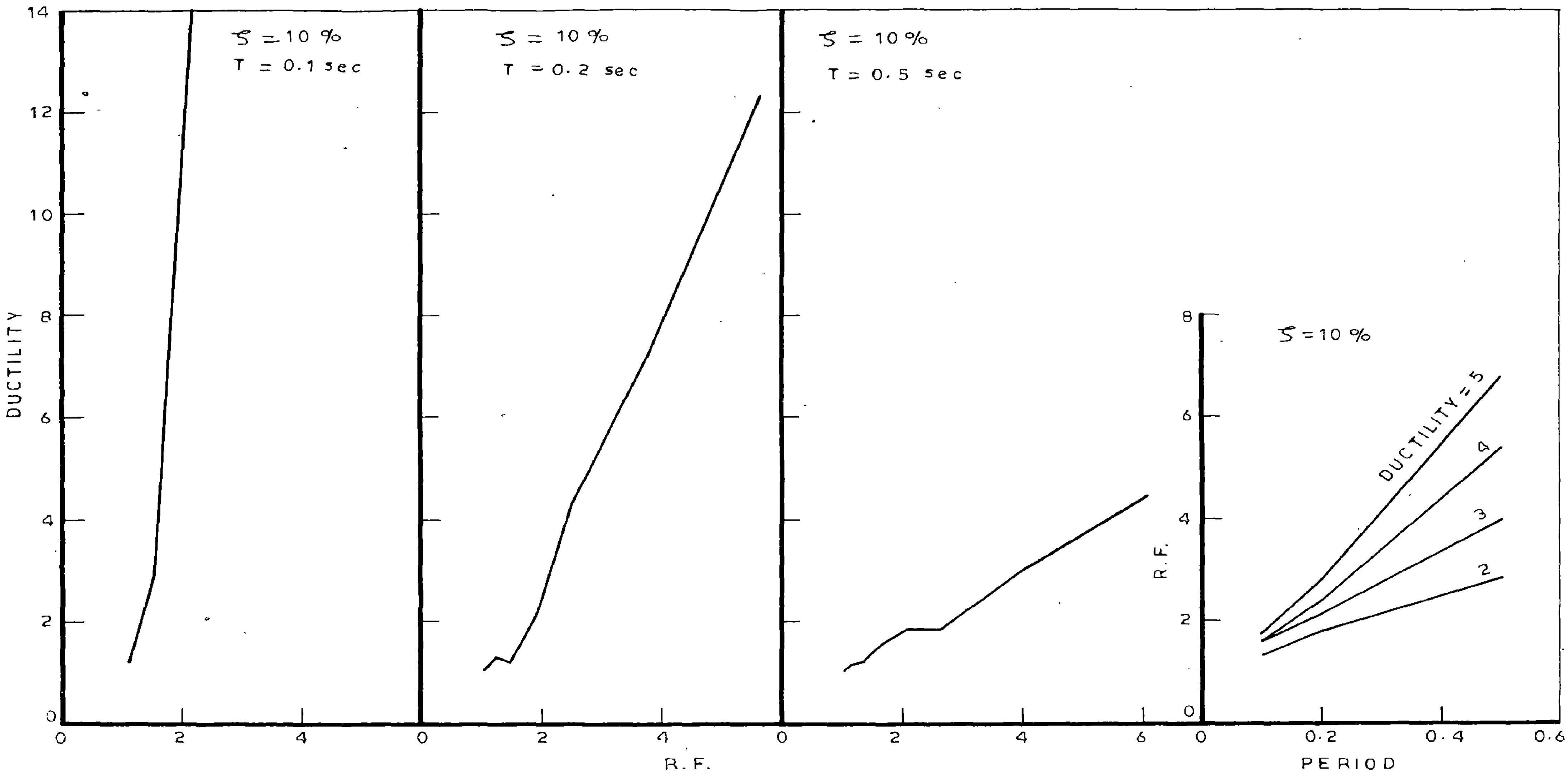

FIG. 3.5-EL CENTRO EARTHQUAKE

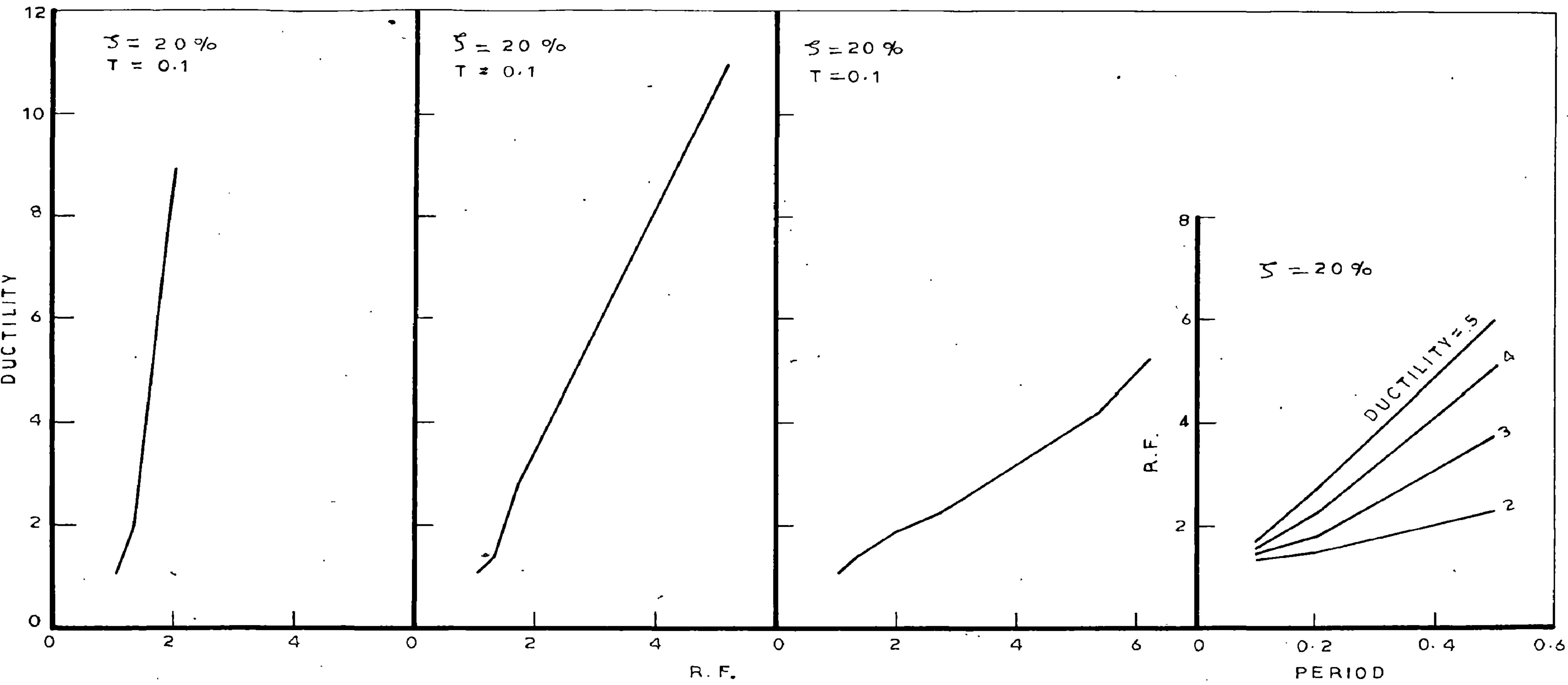

FIG. 3.6 – EL CENTRO EARTH QUAKE

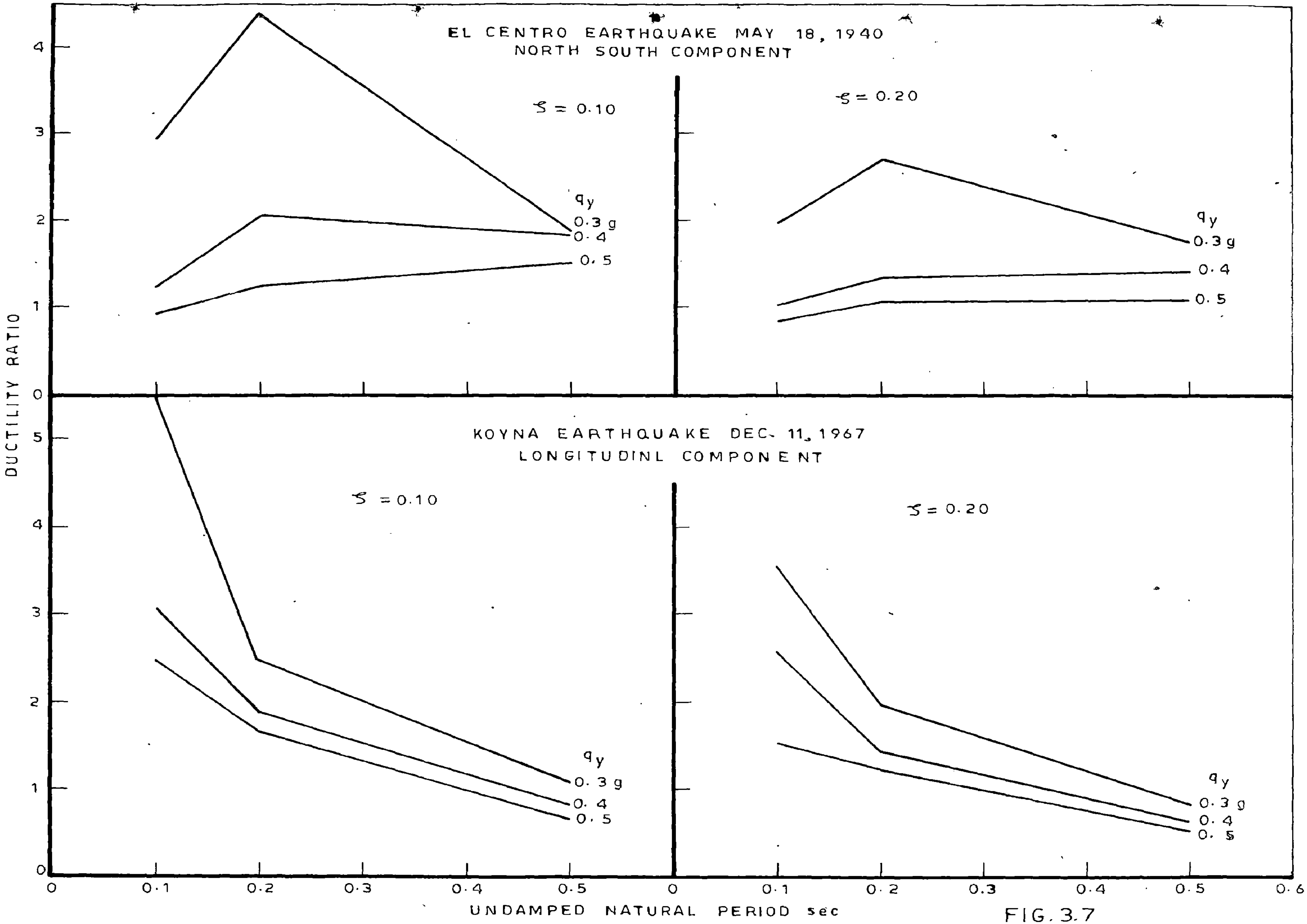
EL CENTRO EARTHQUAKE MAY 18, 1940
NORTH SOUTH COMPONENT
ξ = 0.10
ξ = 0.20
qy
0.3 g
0.4
0.5
KOYNA EARTHQUAKE DEC. 11, 1967
LONGITUDINL COMPONENT
DUCTILITY RATIO
UNDAMPED NATURAL PERIOD sec

FIG. 3.7

CHAPTER IV

SCOPE OF FURTHER WORK IN THE PRESENT STUDY

The primary idea behind the present study being undertaken is to get an insight into the strain behaviour of the structural material with increasing load. A relationship between deflection ductility and strain ductility is indeed, obtained. However, there are many other aspects of the problem which are yet to be studied. In the following pages, a discussion of these is presented.

4.1 In the present study, the behaviour of a rigid jointed, fixed base single storey portal frame is examined. The beam is supposed to be infinitely rigid. It implies that the moment at the top and bottom of a column is always equal and therefore there is simultaneous yielding at both of these points. Is it always the case ? The answer is no. In practice, ratio of moment of inertia of beam and the column denoted by I_b and I_c respectively, is seldom equal to infinity. Referring to Fig. 2.4(a) and using slope deflection equations, one can arrive at the following expression :

$$\frac{M_{BA}}{M_{AB}} = \frac{18\, k_1^2\, k_2^2 + 3\, k_1 .\, k_2}{18\, k_1^2\, k_2^2 + 9\, k_1 .\, k_2 + 1} \qquad 4.1$$

in which,

$$k_1 = \frac{I_b}{I_c}$$

$$k_2 = \frac{h_c}{L_b}$$

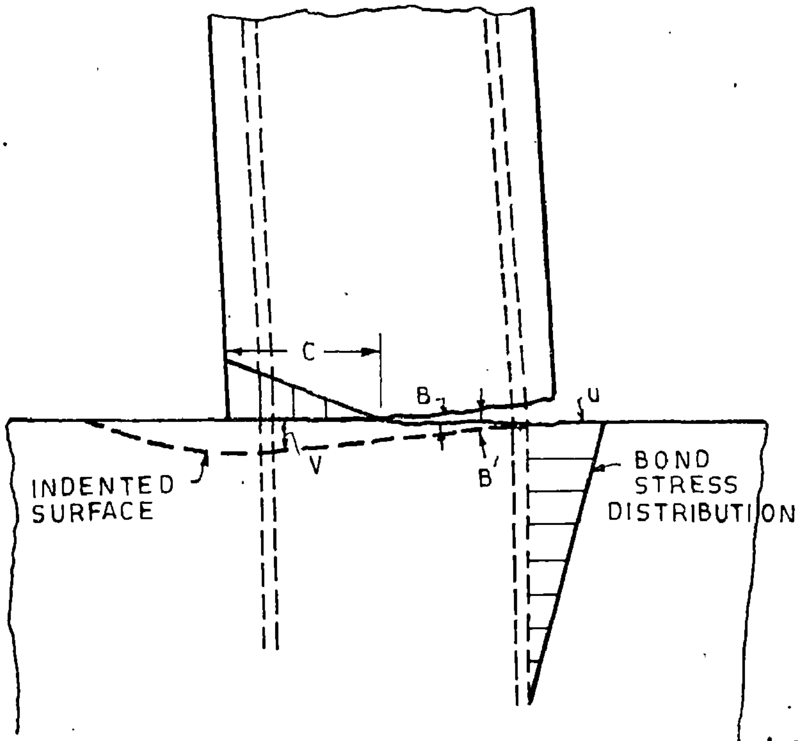

a _ CONTRIBUTION OF BOND SLIP AND 'INDENTATION' TO THE TOTAL DISPLACEMENT YIELD

(a)

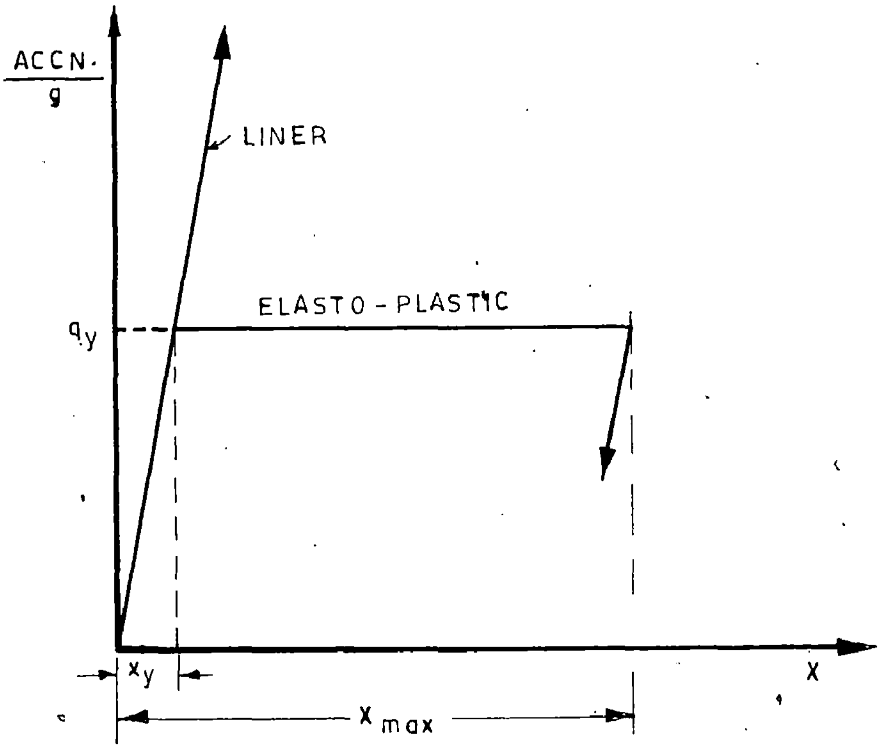

(b)

FIG. 4.1

M_{BA} = moment at the top of column AB

M_{AB} = moment at the bottom of column AB.

As an example, let us take $k_2 = 1$ and $k_1 = 2$. Substituting in Equation 4.1 and simplifying, we get,

$$\frac{M_{BA}}{M_{AB}} = \frac{6}{7} = 0.8571$$

$$\therefore \quad M_{BA} = 0.8571\ M_{AB}$$

With the increase in lateral load, there shall be a stage when M_{AB} will become equal to the yield moment of the column section M_y. At this stage, though the point A has started yielding, at point B, moment is less than M_y and is equal to 0.8571 M_y. On further increasing the load, M_{BA} will ultimately become equal to M_u, the ultimate moment of the column section. The moment at B at this stage may or may not reach M_y, depending upon the ratio k_1. But its value can be assessed. Similarily, the values of the moments at points C and D at each stage can also be assessed.

As soon as any of the four critical sections has yielded, Equation 4.1 is no longer applicable. Since, however, the values of M_y and M_u for a section can be precisely estimated, a new equation of the form of Equation 4.1 can be written using the slope-deflection method. With the help of this equation and by giving incremental increase in the moment of the yielded sections beyond M_y and upto M_u, complete moment diagram history for the column at each stage of loading can be drawn. From the $M - \phi$ diagram, the corresponding curvatures can be obtained. Then using the method indicated in Chapter II, expressions for calculating the lateral deflections at each stage of loading can be obtained.

4.2 In addition to the contribution of curvature to displacement, there are three other effects which contribute to the displacement :

1. displacement arising from shear deformations,
2. displacement caused by the "indentation" of the concrete stress block in the bottom and top girders, and
3. displacement caused by the concentrated rotation which takes place at the "fixity" points of the columns due to the slippage of the reinforcement along the anchorage length.

In the following, expressions will be given for each one of these effects:

1. The deflection caused by the shear deformation is given by

$$x_1 = \frac{1.2 \, P h_c}{2AG} \qquad 4.2$$

in which

P = $4 M/h_c$, shear force acting on both columns

A = gross sectional area

G = shear modulus of concrete assumed equal to $E_c/2.30$.

2. The meaning of "indentation" of concrete stress block is illustrated in Fig. 4.1(a). Treating the bottom and the top girders as elastic half spaces and replacing the triangular stress block by an equivalent uniform distribution and assuming that the indentation does not extend beyond the tensile reinforcement, the following expression gives the value of the vertical depression at the middle of the equivalent uniform distribution (Timoshenko and Goodier, 1951, pp. 96).

$$v = \frac{2\bar{q}}{\pi E_c} \left(\frac{c}{2} \log \frac{d-c/2}{c/2} + \frac{c}{2} \log \frac{d-c/2}{c/2} \right) + \frac{1-\nu}{\pi E_c} \bar{q}\, c \qquad 4.3$$

in which

$\bar{q}$ = equivalent uniform stress

ν = Poisson's ratio for concrete.

The angle θ' can then be found from

$$\theta' = \frac{v}{d-c/2} \qquad 4.4$$

The contribution of the indentation to the total deflection then becomes

$$x_2 = h_c \theta'$$ 4.5

3. The final additional component of the calculated deflection is assumed to have been caused by the slip of the tensile reinforcement along its embedded length. The slip is calculated based on the assumption of a linear distribution of bond stress along the development length as indicated in Fig. 4.1(a). The development length is found from the expression

$$l = \frac{Df_y}{4u}$$ 4.6

in which

D = diameter of the bar

u = unit bond stress.

The elongation at the location of the crack then becomes

$$dl = \frac{l f_y}{2 E_s}$$ 4.7

in which

dl = elongation of the bar at the level of the horizontal crack.

It is assumed that the width of the crack at the same location is equal to dl, than angle θ (Fig. 4.1(a)) is given by

$$\theta = \frac{dl}{d-c}$$ 4.8

The contribution of the slip to the total deflection then becomes

$$x_3 = h_c \theta \qquad 4.9$$

The total displacement is then found from the following expression

$$x_y = x_b + x_1 + x_2 + x_3$$

in which

x_b = deflection contributed by the bending evaluated by integrating the curvature due to bending over the height of the column;

In the present study above mentioned three effects are not included. It should be noted that first and second effects are directly proportional to the moment of the section. It means that by including these effects, the value of displacement in the post elastic range will be affected more than the value of displacement at yield. And, therefore, the actual value of ductilities will be somewhat higher than those obtained in the present study.

4.3 Lastly, it is clear that the present study is purely theoretical in nature. There is a strong need to examine the validity of the conclusions drawn in this study. Unless that is done, designers would be sceptical in applying these results directly to buildings.

CHAPTER V

SUMMARY OF RESULTS AND CONCLUSIONS

Following conclusions are drawn on the basis of present investigation regarding the inelastic behaviour of reinforced concrete frames during earthquake.

1. M - ϕ diagram for a given cross-section remains more or less, unaffected by assuming that concrete does not carry any tension.

2. The axial thrust affects the column moments. Whether the axial thrust will increase or decrease the column moments will depend upon the range of the thrusts and moments considered in the thrust moment interaction diagram.

3. Deflection ductility of the order of 5 is never achieved. The maximum ductility achieved by the structure is of the order of 3. However, even at this value of deflection ductility, the corresponding strain ductility in the reinforcement is of the order of 20.

4. For the same strain ductility, deflection ductility decreases with increasing percentage of steel.

5. Richer the mix, more is the deflection ductility attained by a structure for the same amount of strain ductility.

6. A change in values of the ultimate strain of concrete and the strain at which compressive stress is maximum do not affect the deflection ductility of the structure to any appreciable amount.

7. The reduction factor always increases with an increase in ductility for a given damping and given time period of the system.

8. The effect of ductility on reduction factor is large for larger periods.

9. The reduction factor is very closely associated with the ground motion.

10. For a particular period and damping , the ductility ratio is higher for lower yield levels.

The present study brings out the fact that there is a strong need to examine the strain behaviour of the structural materials while recommending a particular value of ductility. In practice, a ductility of the order of 5 will probable never be achieved as the concrete will be crushed at a value of ductility of the order of 3. Even at this value of deflection ductility the strain in the reinforcement will be about 20 times its yield strain. It is, therefore, concluded that for a strain ductility of the order of 7 in reinforcement, the value of deflection ductility is of the order of 2 for the structures examined in the present study.

From the study of dynamic response of structures in inelastic range, it is concluded that for obtaining the value of minimum yield level and reduction factor for designing a structure for a particular earthquake, the actual accelerogram of the earthquake should be analysed.

SELECTED REFERENCES

1. Brijesh Chandra, "Study of Inelastic Response of Multistorey Frames During Earthquakes", Ph.D. Thesis, Deptt. of Civil Engineering, University of Roorkee, June 1971.

2. Polat Gulkan, and Mete, A., Sozen, "Response and Energy Dissipation of Reinforced Concrete Frames Subjected to Strong Base Motions", A report of the University of Illinois, May 1971.

3. Robert D. Hanson, "Post-Elastic Dynamic Response of Mild Steel Structures", a report of the California Institute of Technology, 1965.

4. S.S. Saini, "Dynamic Response of Nonlinear Structures", M.E. Thesis, Department of Civil Engineering, University of Roorkee, February 1966.

APPENDIX A

PROGRAMME FOR MOMENT-CURVATURE DIAGRAM

```
      DIMENSION C(4)
  675 READ 201,ECAPS,FCBAR,ECULT,ENOT,ESUBY,ACURY,A,P
      READ 299,W,R,D,HBYS,HC,DB,G
  201 FORMAT(8E10.4)
  299 FORMAT(8F10.3)
  202 FORMAT(6HECAPS=,E10.4/6HFCBAR=,E10.4/6HECULT=,E10.4/5HENOT=,E10.4/
     12HP=,F8.4/2HG=,F8.4/2HA=,F8.4/2HW=,E10.4/7HB BY D=,F8.4/2HD=,F8.4/
     212HHT. BY SPAN=,E10.4/7HHEIGHT=,E10.4/3HDB=,F8.4/9HACCURACY=,E10.4
     3/6HESUBY=,E10.4)
  301 FORMAT(//37HPROGRESSIVE ROOTS FROM CUBIC OF ESUBC)
  302 FORMAT(15HVALUES AT YIELD)
  303 FORMAT(6HESUBC=,E10.4/7HMOMENT=,E10.4/4HPHI=,E10.4/
     16HESBAR=,E10.4/5HN.A.=,E10.4/2HJ=,E10.4)
  304 FORMAT(6HFACTOR,5X,5HESUBC,5X,5HESUBS,5X,5HESBAR,4X,6HMOMENT,5X,
     13HPHI,5X,4HN.A.,7X,1HJ)
  305 FORMAT(F6.2,7E10.4)
  306 FORMAT(22HFACTOR IS FOR DIVISION)
  307 FORMAT(28HFACTOR IS FOR MULTIPLICATION)
  308 FORMAT(26HRESULTS FOR TENSION COLUMN)
  309 FORMAT(30HRESULTS FOR COMPRESSION COLUMN)
      PUNCH202,ECAPS,FCBAR,ECULT,ENOT,P,G,A,W,R,D,HBYS,HC,DB,ACURY,ESUBY
      L=1
   82 PUNCH 309
      GO TO 678
   81 PUNCH 308
  678 ECOLD=0.
      RHS=0.
      ESUBC=0.
      ESUBS=ESUBY
      TSBAR=P*ECAPS*ESUBY
      CSBAR=G*TSBAR
      PUNCH 301
 1000       CALL C01(FCBAR,ENOT,G,P,ECAPS,A,ESUBS,TSBAR,C)
      C(4)=C(4)-RHS*(ESUBC+ESUBS)
C     C01 GENERATES ZERO RHS
      CALL CUBIC(C,IC,ROOT)
      IF(IC)1028,100,1028
  100 ESUBC=ROOT
      KODE=1
      ESBAR=(1.-A)*ESUBC-A*ESUBS
      IF(ESBAR-ESUBY)1,2,2
    2 KODE=0
            CALL C02(FCBAR,ENOT,CSBAR,TSBAR,ESUBS,C)
      C(4)=C(4)-RHS*(ESUBC+ESUBS)
      CALL CUBIC(C,IC,ROOT)
      IF(IC)1028,101,1028
  101 ESUBC=ROOT
    1       CALL C0100(FCBAR,ESUBC,ENOT,ESUBS,KODE,G,P,ECAPS,A,ESUBY,HC,
```

```
     1DB,W,R,D,HBYS,L,EN,ZJ,RHS,ZMB)
      PUNCH201,ESUBC
      PCTG=((ESUBC-ECOLD)/ESUBC)
      PCTG=ABSF(PCTG)
      IF(PCTG-ACURY)1001,1001,1002
 1002 ECOLD=ESUBC
      GO TO 1000
 1001 PHI=(ESUBC+ESUBS)/D
      RHSYD=RHS
      ECY=ESUBC
      PUNCH 302
      PUNCH303,ESUBC,ZMB,PHI,ESBAR,EN,ZJ
C     PRESCRIBING VALUES OF ESUBC
      IF(ESUBC-ECULT)1009,1016,1016
 1009 READ299,FLAST
      PUNCH 306
      PUNCH 304
 1010 READ299,FACTR
      ESOLD=0.
      ESUBC=ECY/FACTR
      RHS=0.
      ESUBS=0.
      CC=FCBAR*ESUBC*ESUBC/ENOT
      CC=CC*(1.-ESUBC/(3.*ENOT))
 1004       CALL CC3(P,ECAPS,A,G,CC,ESUBC,C)
      C(3)=C(3)-RHS*(ESUBC+ESUBS)
      CALL QUAD(C,IC,ROOT)
      IF(IC)1028,102,1028
  102 ESUBS=ROOT
      KODE=1
      ESBAR=(1.-A)*ESUBC-A*ESUBS
      IF(ESBAR-ESUBY)10,11,11
   11 KODE=0
            CALL CO4(P,ECAPS,CSBAR,ESUBC,CC,C)
      C(3)=C(3)-RHS*(ESUBC+ESUBS)
      CALL QUAD(C,IC,ROOT)
      IF(IC)1028,103,1028
  103 ESUBS=ROOT
   10       CALL CO100(FCBAR,ESUBC,ENOT,ESUBS,KODE,G,P,ECAPS,A,ESUBY,HC
     1DB,W,R,D,HBYS,L,EN,ZJ,RHS,ZMB)
      PCTG=(ESUBS-ESOLD)/ESUBS
      PCTG=ABSF(PCTG)
      IF(PCTG-ACURY)1003,1003,1005
 1005 ESOLD=ESUBS
      GO TO 1004
 1003 PHI=(ESUBS+ESUBC)/D
      PUNCH 305,FACTR,ESUBC,ESUBS,ESBAR,ZMB,PHI,EN,ZJ
      IF(FACTR-FLAST)1010,1011,1011
 1011 FACTR=1.
      ESOLD=0.
```

```
      PUNCH 307
      PUNCH 304
      RHS=RHSYD
      ESUBS=ESUBY
 1015 ESUBC=ECY*FACTR
      IF(ESUBC-ECULT)1025,1026,1026
 1026 ESUBC=ECULT
 1025 CC=FCBAR*ESUBC*ESUBC/ENOT
      CC=CC*(1.-ESUBC/(3.*ENOT))
 1030 CALL C05(G,P,A,ECAPS,ESUBC,TSBAR,CC,C)
      C(3)=C(3)-RHS*(ESUBC+ESUBS)
      CALL QUAD(C,IC,ROOT)
      IF(IC)1028,104,1028
  104 ESUBS=ROOT
      KODE=1
      ESBAR=(1.-A)*ESUBC-A*ESUBS
      IF(ESBAR-ESUBY)15,16,16
   16 ESUBS=CC/(RHS-CSBAR+TSBAR)-ESUBC
      KODE=0
   15       CALL C0100(FCBAR,ESUBC,ENOT,ESUBS,KODE,G,P,ECAPS,A,ESUBY,HC,
     1DB,W,R,D,HBYS,L,EN,ZJ,RHS,ZMB)
      PCTG=(ESUBS-ESOLD)/ESUBS
      PCTG=ABSF(PCTG)
      IF(PCTG-ACURY)1021,1021,1022
 1022 ESOLD=ESUBS
      GO TO 1030
 1021 PHI=(ESUBS+ESUBC)/D
      PUNCH 305,FACTR,ESUBC,ESUBS,ESBAR,ZMB,PHI,EN,ZJ
      IF(ESUBC-ECULT)1027,1029,1029
 1027 FACTR=FACTR+0.5
      GO TO 1015
 1016 PUNCH1017
 1017 FORMAT(55HCONC STRAIN IS ULT WHEN STEEL YIELDS                   )
      GO TO 1029
 1028 PUNCH 1031
 1031 FORMAT(14HROOT IS ABSURD)
 1029 L=-L
      IF(L)81,81,84
   84 GO TO 675
  676 STOP
      END
      SUBROUTINE CUBIC(C,IC,ROOT)
      DIMENSION C(4),R(1)
      IP=2
      A0=C(4)/C(1)
      A1=C(3)/C(1)
      A2=C(2)/C(1)
      EX=1./3.
      IF(C(4))30,29,30
   29 R(1)=0.
      GOTO 1034
```

```
   30 Q=(A0-A2*A1/3.+2.*A2*A2*A2/27.)/2.
      IF(Q)1010,1008,1014
 1008 Z=0.
      GO TO 1032
 1010 Q=-Q
      IP=1
 1014 P=(A1-A2*A2/3.)/3.
      P3=P*P*P
      Q2=Q*Q
      PQ=P3+Q2
      IF(PQ)31,32,33
   31 Z=-2.*SQRTF(-P)*COSF(ATANF(SQRTF(-PQ)/Q)/3.)
      GO TO 1028
   32 Z=-2.*Q**EX
      GO TO 1028
   33 SPQ=SQRTF(PQ)
      IF(P)34,35,36
   34 Z=-(Q+SPQ)**EX-(Q-SPQ)**EX
      GO TO 1028
   35 Z=-(2.*Q)**EX
      GO TO 1028
   36 Z=(SPQ-Q)**EX-(SPQ+Q)**EX
 1028 GO TO (1030,1032),IP
 1030 Z=-Z
 1032 R(1)=Z-A2/3.
 1034 C(2)=C(2)+R(1)*C(1)
      C(3)=C(3)+R(1)*C(2)
      CALL QUAD(C,IC,ROOT)
      IF(IC)61,62,61
   61 IF(R(1))63,64,64
   64 IC=0
      ROOT=R(1)
      GO TO 63
   62 IF(R(1))63,65,65
   65 IF(ROOT-R(1))63,63,66
   66 ROOT=R(1)
   63 RETURN
      END


      SUBROUTINE QUAD(C,IC,ROOT)
      DIMENSION C(3)
      A=C(1)
      B=C(2)
      AC=C(3)
      IF(A)81,82,81
   82 ROOT=-AC/B
      GO TO 44
   81 D2=B*B-4.*A*AC
      F=-B/(2.*A)
      IF(D2)45,42,43
   42 ROOT=F
```

```
      GO TO 44
   43 D=SQRTF(D2)/(2.*A)
      ROOT1=F+D
      ROOT2=F-D
      IF(ROOT1)51,52,52
   51 IF(ROOT2)45,62,62
   52 IF(ROOT2)60,60,63
   63 IF(ROOT1-ROOT2)60,60,62
   60 ROOT=ROOT1
      GO TO 46
   62 ROOT=ROOT2
      GO TO 46
   44 IF(ROOT)45,45,46
   45 IC=1
      ROOT=1000.
      GO TO 47
   46 IC=0
   47 RETURN
      END
      SUBROUTINE CO1(FCBAR,ENOT,G,P,ECAPS,A,ESUBS,TSBAR,C)
      DIMENSION C(4)
      C(1)=-FCBAR/(3.*ENOT*ENOT)
      C(2)=(FCBAR/ENOT+G*P*ECAPS*(1.-A))
      C(3)=G*P*ECAPS*(1.-2.0*A)*ESUBS-TSBAR
      C(4)=-TSBAR*ESUBS-G*P*ECAPS*A*ESUBS*ESUBS
      RETURN
      END
      SUBROUTINE CO2(FCBAR,ENOT,CSBAR,TSBAR,ESUBS,C)
      DIMENSION C(4)
      C(1)=-FCBAR/(3.*ENOT*ENOT)
      C(2)=FCBAR/ENOT
      C(3)=CSBAR-TSBAR
      C(4)=C(3)*ESUBS
      RETURN
      END
      SUBROUTINE CO3(P,ECAPS,A,G,CC,ESUBC,C)
      DIMENSION C(3)
      C(1)=-P*ECAPS*(1.+A*G)
      C(2)=P*ECAPS*ESUBC*((-2.*A*G-1.)
      C(3)=CC+G*P*ECAPS*(1.-A)*ESUBC*ESUBC
      RETURN
      END
      SUBROUTINE CO4(P,ECAPS,CSBAR,ESUBC,CC,C)
      DIMENSION C(3)
      C(1)=-P*ECAPS
      C(2)=CSBAR-P*ECAPS*ESUBC
      C(3)=CC+CSBAR*ESUBC
      RETURN
      END
      SUBROUTINE CO5(G,P,A,ECAPS,ESUBC,TSBAR,CC,C)
```

```
      DIMENSION C(3)
      C(1)=-G*P*A*ECAPS
      C(2)=G*P*ECAPS*(1.-2.*A)*ESUBC-TSBAR
      C(3)=CC-TSBAR*ESUBC+G*P*ECAPS*(1.-A)*ESUBC*ESUBC
      RETURN
      END
      SUBROUTINE CO100(FCBAR,ESUBC,ENOT,ESUBS,KODE,G,P,ECAPS,A,ESUBY,HC,
     1DB,W,R,D,HBYS,L,EN,ZJ,RHS,ZMB)
      CCBAR=FCBAR*ESUBC*ESUBC
      CCBAR=CCBAR*(1.-ESUBC/3.*ENOT)
      CCBAR=CCBAR/(ENOT*(ESUBC+ESUBS))
      AL=L
      IF(KODE)3,4,3
    3 CSBAR=G*P*ECAPS*((1.-A)*ESUBC-A*ESUBS)
      GO TO 5
    4 CSBAR=G*P*ECAPS*ESUBY
    5 EN=ESUBC/(ESUBC+ESUBS)
      CNUM=1.-(3.*ESUBC/(8.*ENOT))
      CDEN=1.-(ESUBC/(3.*ENOT))
      EC=0.666667*EN*CNUM/CDEN
      ZJ=1.+EC-EN
      ZM=CCBAR*ZJ+CSBAR*(1.-A)
      Z=(HC+DB)/HC
      ZMB=ZM*Z
      RHS=(W/(R*D*D))+2.*AL*ZMB*D*HBYS/HC
      RETURN
      END
```

```
      PROGRAMME FOR OBTAINING DUCTILITIES OF STRAIN AND DEFLECTION
C  C  CALCULATION OF DUCTILITY CURVES   RAV PRK   16030
      DIMENSION ZM(10),PHI(10),STN(10)
      READ 10,NDATA
      DO 1 N=1,NDATA
      PUNCH 15,N
      READ 11,P,G,R,D,HBS,HC
      PUNCH 16,P,G,R,D,HBS,HC
      READ 10,NX
      READ 11,(ZM(I),I=1,NX)
      READ 11,(PHI(I),I=1,NX)
      READ 11,(STN(I),I=1,NX)
      READ 11,ZMY,PHIY,STNY
      PUNCH 19,ZMY,PHIY
   10 FORMAT(I5)
   11 FORMAT(8E10.4)
      PY=(ZMY*R*D*D*D)/(250.*HC)
      DELY=PHIY*HC*HC/12.
      PUNCH 17,PY
      PUNCH 18,DELY
      PUNCH 14
      DO 1 I=1,NX
      A=ZM(I)
      B=PHI(I)
      ZMR=A/ZMY
      P=PY*ZMR
      PHIR=B/PHIY
      STNR=STN(I)/STNY
            CALL DELTA(HC,ZMY,A,PHIY,B,DELY,DELR,DEL)
      PUNCH 12,P,DEL,ZMR,PHIR,STNR,DELR
    1 CONTINUE
   12 FORMAT(6(E10.4,3X))
   14 FORMAT(4X,1HP,8X,10HDEFLECTION,3X,3HZMR,10X,4HPHIR,9X,4HSTNR,9X,
     14HDELR)
   15 FORMAT(///12HDATA SET NO.,I2)
   16 FORMAT(2HP=,E10.4,1H,,2HG=,E10.4,1H,,2HR=,E10.4,1H,,2HD=,E10.4,
     11H,,4HHBS=,E10.4,1H,,3HHC=,E10.4)
   17 FORMAT(/11HP AT YIELD=,E10.4,6HTONNES)
   18 FORMAT(20HDEFLECTION AT YIELD=,E10.4,4HCMS.)
   19 FORMAT(4HZMY=,E10.4,1H,5HPHIY=,E10.4)
      STOP
      END
      SUBROUTINE DELTA(HC,ZMY,A,PHIY,B,DELY,DELR,DEL)
      QL2=HC*ZMY/(2.*A)
      QL1=0.5*HC-QL2
      TH2=0.5*PHIY*QL2
      Y2=PHIY*QL2*QL2/3.
      TH1=0.5*QL1*(B+PHIY)
      Y1=QL1*QL1*(2.*B+PHIY)/6.
```

```
TT=TH1+TH2
DEL=2.*(QL2*SINF(TT)-Y2*COSF(TT)+Y1)
DELR=DEL/DELY
RETURN
END
```

NOTATIONS

The symboles used in the present text are defined where they first appear. For quick reference the notations are given below in alphabatical order:

C_c	=	Compressive force in the concrete
C_s	=	Compressive force in compression steel
E_s	=	Modulus of elasticity of steel
I_b	=	Moment of inertia of the beam
I_c	=	Moment of inertia of the column
M	=	Moment
M_b	=	Moment in the beam
Nd	=	Depth of nutral axis
P	=	Leteral load at the top of the portal frame
R	=	Restoring force function
T	=	Time period of the system
T_s	=	Tensile force in the tensile steel
W	=	Direct thrust in the column
X	=	Lateral deflection
a	=	Acceleration
ad	=	Depth of compression steel from top
b	=	Width of the section
c	=	Damping
	=	Distance of the C.G. of compressive force of concrete from neutral axis

d	=	Effective depth of the section
d'	=	Distance between compressive and tensile steel
d_b	=	Total depth of the beam
e	=	Strain
e_c	=	Strain in the top fibre of concrete
e_o	=	Strain in concrete at which compressive stress is maximum
e_s	=	Strain in steel
e'_s	=	Strain in compressive steel
f	=	Stress
f'_c	=	Maximum compressive stress in concrete
g	=	Acceleration due to gravity
h_c	=	Height of the column (clear)
k_1	=	Ratio of moment of inertias of beam and column
k_2	=	Ratio of height and span of the frame
m	=	Mass
p	=	Percentage of tensile steel
p'	=	Percentage of compressive steel
q_y	=	Yield level
t	=	Time parameter
x	=	Relative displacement of system with respect to ground
y	=	Ground displacement
ϕ	=	Curvature
ρ	=	Damping as a percentage of critical.